SANDIA REPORT

SAND2015-0317
Unlimited Release
Printed January 2015

Aleph Field Solver Challenge Problem Results Summary

Russell Hooper and Stan Moore

Prepared by
Sandia National Laboratories
Albuquerque, New Mexico 87185 and Livermore, California 94550

Sandia National Laboratories is a multi-program laboratory managed and operated by Sandia Corporation, a wholly owned subsidiary of Lockheed Martin Corporation, for the U.S. Department of Energy's National Nuclear Security Administration under contract DE-AC04-94AL85000.

Sandia National Laboratories

Issued by Sandia National Laboratories, operated for the United States Department of Energy by Sandia Corporation.

Available to DOE and DOE contractors from
U.S. Department of Energy
Office of Scientific and Technical Information
P.O. Box 62
Oak Ridge, TN 37831

Telephone: (865) 576-8401
Facsimile: (865) 576-5728
E-Mail: reports@adonis.osti.gov
Online ordering: http://www.osti.gov/bridge

Available to the public from
U.S. Department of Commerce
National Technical Information Service
5285 Port Royal Rd
Springfield, VA 22161

Telephone: (800) 553-6847
Facsimile: (703) 605-6900
E-Mail: orders@ntis.fedworld.gov
Online ordering: http://www.ntis.gov/help/ordermethods.asp?loc=7-4-0#online

SAND2015-0317
Unlimited Release
Printed January 2015

Aleph Field Solver Challenge Problem Results Summary

Russell Hooper
Multiphysics Applications
Sandia National Laboratories
P.O. Box 5800, MS 1318
Albuquerque, NM 87185-1318
rhoope@sandia.gov

Stan Moore
Multiscale Science
Sandia National Laboratories
P.O. Box 5800, MS 1318
Albuquerque, NM 87185-1318
stamoor@sandia.gov

Abstract

Aleph models continuum electrostatic and steady and transient thermal fields using a finite-element method. Much work has gone into expanding the core solver capability to support enriched modeling consisting of multiple interacting fields, special boundary conditions and two-way interfacial coupling with particles modeled using Aleph's complementary particle-in-cell capability. This report provides quantitative evidence for correct implementation of Aleph's field solver via order-of-convergence assessments on a collection of problems of increasing complexity. It is intended to provide Aleph with a pedigree and to establish a basis for confidence in results for more challenging problems important to Sandia's mission that Aleph was specifically designed to address.

Contents

List of Figures

List of Tables

Summary

A series of challenge problems was used to perform a code verification study for Aleph's finite-element-method (FEM)-based field solver. Aleph's ability to solve each problem correctly was determined by assessing order-of-covergence using refinement of either mesh size Δx or time step size Δt. Table 1 summarizes the observed orders-of-accuracy along with the expected theoretical values. The parameter values reported in the table correspond to expressions for numerical error of the forms $E_{\Delta x} = C_1(\Delta x)^p$ and $E_{\Delta t} = C_2(\Delta t)^q$. The last column indicates whether or not the

Challenge Problem	Key Capability Tested	p Obs.	p Th.	q Obs.	q Th.	Reg. Test
1	Simple Steady State	*	*	-	-	N
2	Constant Source Term	1.996	2.0	-	-	Y
3	Spatially-Dependent Material	1.85	2.0	-	-	Y
4	Thermally-Dependent Material (1-Way Coupling)	1.87	2.0	-	-	Y
5	Simple Transient	-	-	*	*	Y
6	Transient Linear Conduction	-	-	1.02	1.0	Y
7	Analytic Transient Flux BC	-	-	0.992	1.0	Y
8	Physical Conduction into 1D Slab	2.06	2.0	0.98	1.0	Y
9	Particle-Based & Emission Transient Flux BC	-	-	1.11	1.0	Y
10	2D version of problem 2	-	-	2.000	2.0	Y
11	3D Parallel Transient version of problem 6	1.73	2.0	0.98	1.0	Y

Table 1. Aleph field solver challenge problem order-of-convergence summary

challenge problem is included in Aleph's regression test suite. The asterisks indicate challenge problems for which more stringent requirements are used to assess correctness. If correctly implemented, Aleph's FEM solver should exactly capture the known spatial solution to Problem 1, and it does. If Aleph's time integration method is implemented correctly, the transient solution for Problem 5 should be captured exactly, and it is.

We chose this approach to verify correctness of the Aleph code based on current best-practices in verification within computational science and engineering [4]:

> "What is gained by verifying the order-of-accuracy of a PDE code? Briefly, the answer is that a code whose order-of-accuracy has been verified is free of any coding mistakes that prevent one from computing the correct answer."

In summary, Aleph is shown to provide reasonably good agreement with theoretical behavior and can therefore be expected to give credible results for more complex problems using the models and methods considered in this study.

These studies were performed using the Aleph release candidate code base reflected in the tagged version-1.0rc1 in the Aleph subversion repository located at
`svn+ssh://development.sandia.gov/usr/local/svn/arcmodel/aleph/trunk/`.
Meshes were generated using the journal files contained in the Aleph examples directory, `examples/verification/meshes`, along with cubit version 14.1 64 bit Build 390841.

Chapter 1

1D Verification

Aleph embodies a mutually coupled continuum-to-particle capability. Continuum modeling consists of electrostatic potential and transient thermal conduction subject to a rich variety of boundary conditions. To model these, Aleph uses the Finite Element Method (FEM) to solve various expressions of the Poisson equation discretized over 1D, 2D and 3D unstructured mesh domains [2]. The following sections present results for a sequence of increasingly complex challenge problems that together provide strong evidence for the correct implementation of models and solution algorithms in Aleph.

1.1 Problem 1: Trivial Steady Linear Heat Conduction

Perhaps the simplest physical model to consider is that of steady linear heat conduction with fixed boundary temperatures. In the absence of a thermal source, the governing equation is

$$\frac{d^2T}{dx^2} = 0 \tag{1.1}$$

and simple values can be chosen for boundary conditions as

$$\begin{aligned} T(0) &= 0 \\ T(1) &= 1 \end{aligned}$$

This particular problem admits the exact solution $T(x) = x$. The linear FEM basis functions used by Aleph together with default solver settings should produce a discrete numerical solution equivalent to the exact solution limited only by machine precision regardless of the number of elements used to discretize the problem. Two simulations were run using meshes containing 3 elements ($\Delta x = 1/3$) and 1000 elements ($\Delta x = 0.001$). Numerical values at the nodes in the mesh for the latter were exactly in agreement with the analytic result, and numerical values for the former coarse mesh showed only a single difference in the least significant digit associated with representing the value of $2/3$ as a decimal, i.e. $T_{\Delta x=1/3} = [0, 0.333333333333333, 0.666666666666667, 1]$.

1.2 Problem 2: Steady Linear Heat Conduction with Source

The next challenge problem includes a spatially varying source term chosen to admit the analytic solution, $T(x) = m\sin(n\pi x)$ where m and n are adjustable parameters that essentially control solution amplitude and curvature. We apply the Laplace operator of eq. (1.1) to this solution to obtain the corresponding source term used in Aleph. This leads to the following form for this challenge problem:

$$\frac{d^2T}{dx^2} = -mn^2\pi^2\sin(n\pi x) \tag{1.2}$$

with consistent fixed Dirichlet boundary conditions,

$$\begin{aligned} T(0) &= 0 \\ T(1) &= m\sin(n\pi) \end{aligned} \tag{1.3}$$

The presence of the non-zero source term makes this problem more challenging than the previous problem because the piecewise linear FEM solution cannot exactly capture the analytic solution due to the solution curvature. However, the FEM solution should converge to the exact solution as the mesh is refined and should do so as $O(\Delta x^2)$. To assess whether or not Aleph's FEM solver is correct, this problem was solved on a sequence of uniform (constant element size) meshes characterized by $\Delta x = 0.01, 0.005, 0.002, 0.001, 0.0001$. Nominal values for the parameters were used, i.e. $m = 1.4$ and $n = 3.5$. A comparison of numerical and exact solutions for this problem are shown in Figure 1.1 and provide initial evidence of correct convergence behavior. To quantify this, a measure for error in the FEM solutions was computed as the L2-norm of the difference between the FEM solution and the exact solution, i.e. $E \equiv ||T(x) - T_{\Delta x}(x)||_2$. These error values are plotted against the mesh size Δx in Figure 1.2 along with a best-fit to the assumed functional form for discretization error $E = C(\Delta x)^p$. For this challenge problem, Aleph's FEM field solver exhibits an order-of-accuracy of 1.996, which agrees very well with the expected theoretical value of 2.0.

The input files associated with this calculation are in the Aleph repository at `examples/verification/1d/T_only`.

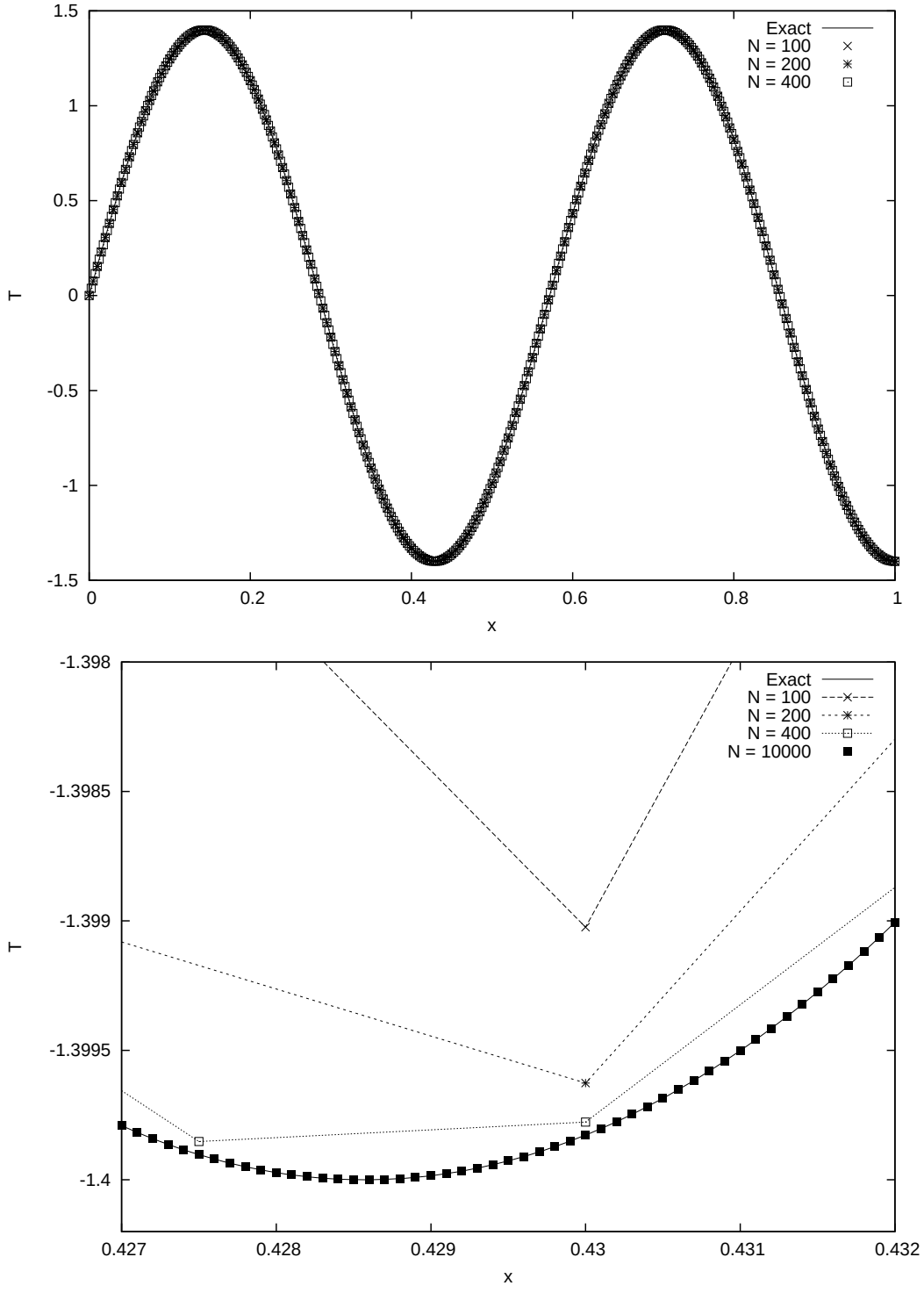

Figure 1.1. Comparison of numerical and exact solutions for various mesh refinement levels for Challenge Problem 2. Mesh spacing Δx is related to number of elements N by $\Delta x = 1.0/N$. The unequal spacing of the errors at $x = 0.43$ reflects the order of convergence quantified in Figure 1.2.

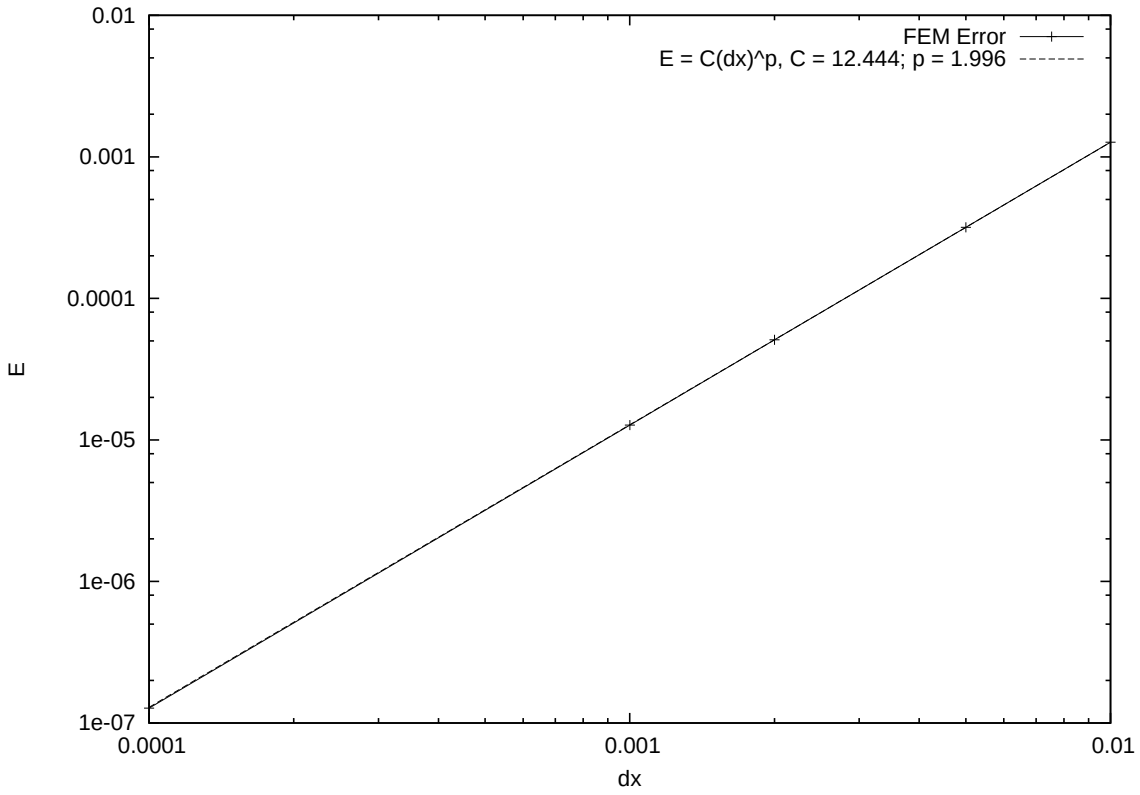

Figure 1.2. Observed order-of-accuracy for Challenge Problem 2. The dashed line is a least-squares fit to the numerical error.

1.3 Problem 3: Electrostatic Potential with Spatially Varying Permittivity

This challenge problem builds on the previous one by introducing a spatially varying material property into the Poisson equation governing the electrostatic potential field V. In this case, we choose to represent the material permittivity ε as follows:

$$\varepsilon = \varepsilon_0 m^2 \sin^2(n\pi x) \tag{1.4}$$

Not coincidentally, this is equivalent to $\varepsilon = \varepsilon_0 T^2$ if we employ the exact solution for the temperature field used in the previous challenge problem. As before, we define an exact solution, this time for the potential, $V = a\cos(b\pi x)$. We then apply the Laplace operator to this exact solution and use the expression for permittivity to generate a corresponding source term. This challenge problem takes the following form:

$$\begin{aligned} \frac{d}{dx}\left(\varepsilon\frac{dV}{dx}\right) &= ab\varepsilon_0 m^2\pi^2[\\ &\quad 2n\sin(n\pi x)\cos(n\pi x)\sin(b\pi x) + \\ &\quad b\sin(n\pi x)\sin(n\pi x)\cos(b\pi x)] \end{aligned} \tag{1.5}$$

The corresponding boundary conditions are:

$$\begin{aligned} V(0) &= a \\ V(1) &= a\cos(b\pi) \end{aligned} \tag{1.6}$$

The coefficients, ε_0, a, b, m and n are arbitrary parameters that specify the exact solution and permittivity.

In addition to exercising variable material properties, this challenge problem also exercises Aleph code infrastructure supporting generalized material models and source terms.

An assessment of Aleph's correctness is achieved as before by performing a sequence of runs on meshes of various refinements and determining discretization error by differencing with exact solution values. This problem requires a finer collection of meshes to be used because of the increased solution curvature associated with the spatially varying permittivity. Meshes consisted of $\Delta x = 0.002, 0.001, 0.0002, 0.0001$, and the following coefficient values were used, $[\varepsilon_0, a, b, m, n] = [1.5, 1.8, 2.5, 1.4, 3.5]$. The exact solution and representative numerical solutions are shown in Figure 1.3, and the order-of-accuracy results are shown in Figure 1.4. This challenge problem exhibits an order-of-accuracy of 1.85, and was deemed satisfactory compared with the theoretical value of 2.0.

The input files associated with this calculation are in the Aleph repository at `examples/verification/1d/V_only`.

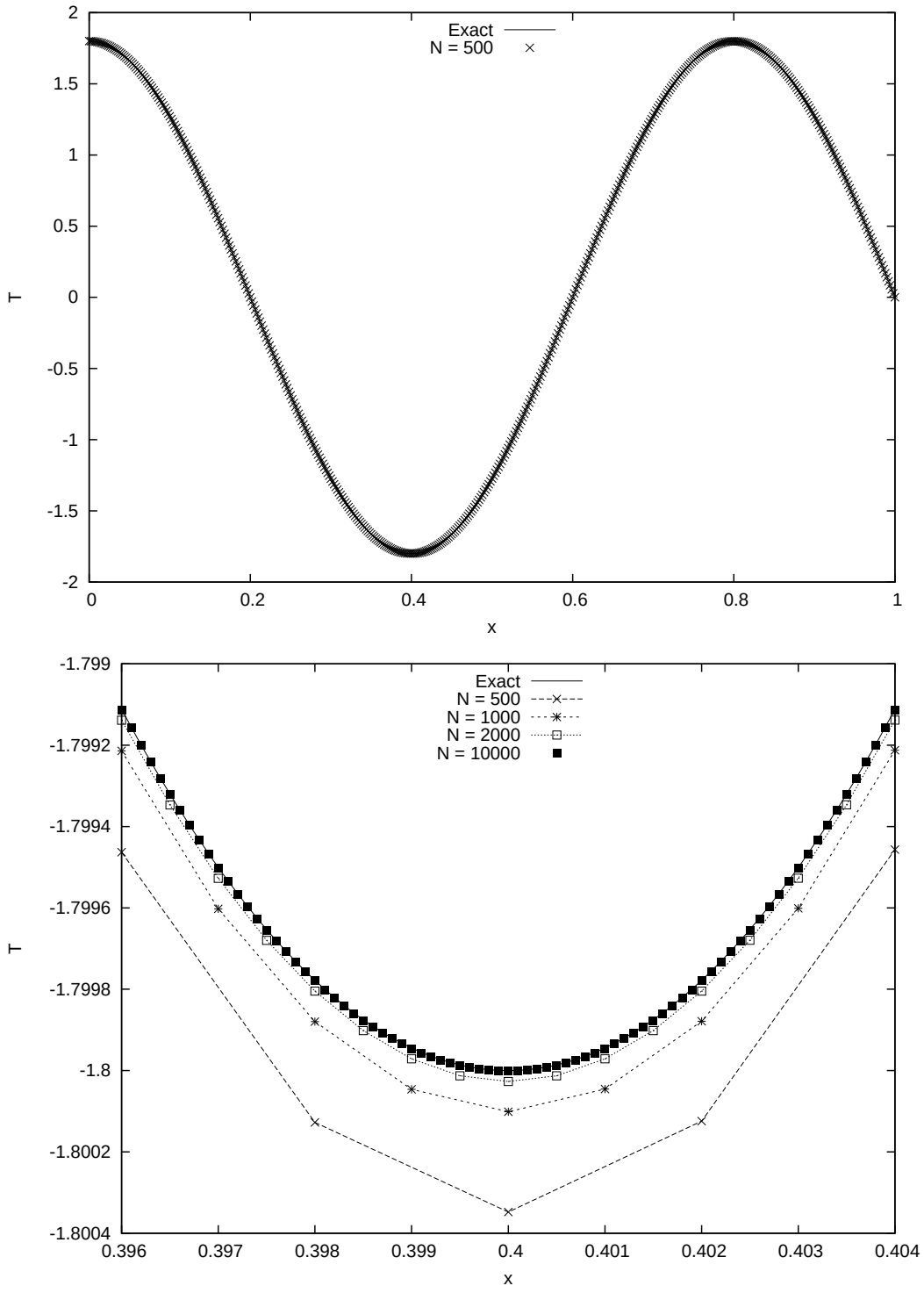

Figure 1.3. Comparison of numerical and exact solutions for various mesh refinement levels for Challenge Problem 3. Mesh spacing Δx is related to number of elements N by $\Delta x = 1.0/N$. The unequal spacing of the errors at $x = 0.40$ reflects the order of convergence quantified in Figure 1.4.

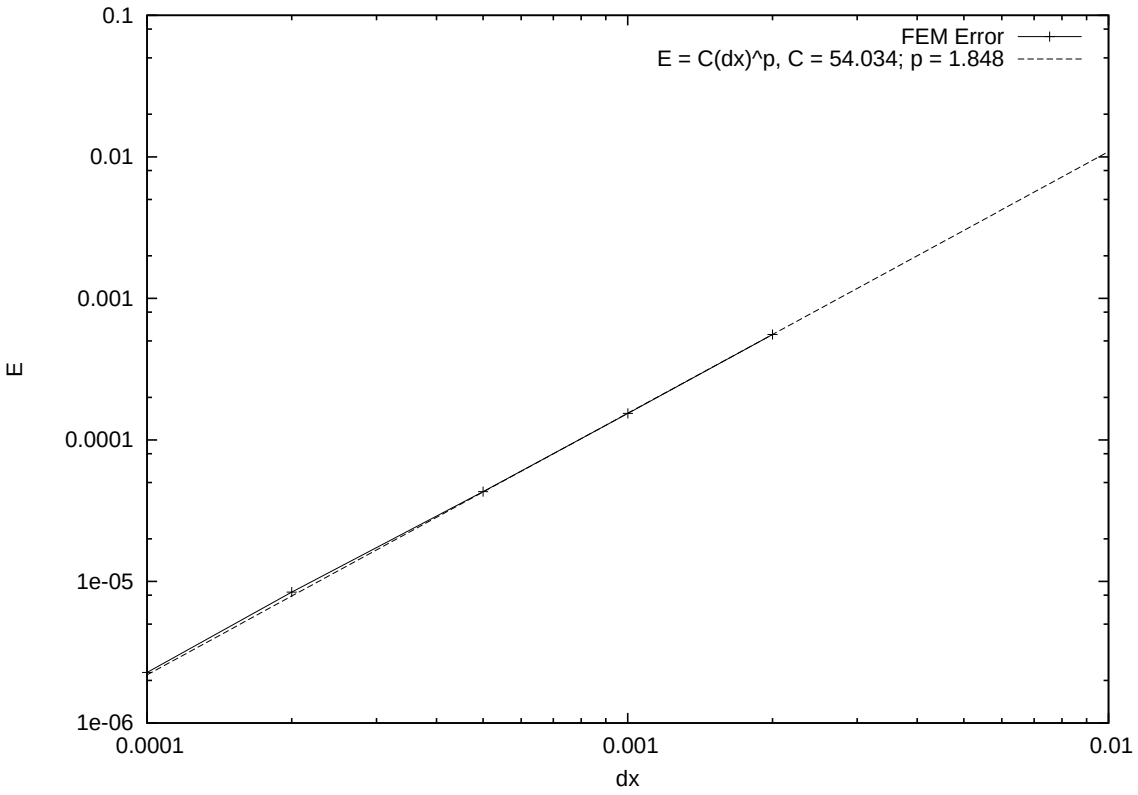

Figure 1.4. Observed order-of-accuracy for Challenge Problem 3. The dashed line is a least-squares fit to the numerical error.

1.4 Problem 4: One-Way Coupled Steady Temperature and Electrostatic Potential

This challenge problem combines the previous two to demonstrate Aleph's ability to correctly drive a coupled multiphysics problem. In particular, the thermal problem of eqs. (1.2) and (1.3) is solved and the resulting temperature field is then used to compute the permittivity as

$$\varepsilon = \varepsilon_0 T^2 \tag{1.7}$$

This permittivity is used to solve the same electrostatic problem defined in eqs. (1.5) and (1.6).

The important aspects of this challenge problem mainly concern code and solver infrastructure required to construct, configure and orchestrate multiple field solvers. Aleph underwent several iterations of implementation and debugging to arrive at a credible capability that also includes the ability to pass field data among solvers (which can be applied to different parts of the domain) and the ability to utilize passed field data in the computation kernels of dependent field solvers. When performed properly, the results for this challenge problem should encompass those of the previous two with very similar mesh convergence behavior. Note that some slight differences are expected due to the way field data is passed and used within dependent solver assembly kernels, e.g., mapping node values to Gauss points introduces differences due to interpolation. Exact and numerical solutions are shown in Figure 1.5.

The order-of-accuracy results for both the temperature and electrostatic potential fields are shown in Figure 1.6. This challenge problem exhibits orders-of-accuracy of 2.00 and 1.87 for temperature and potential fields, respectively, and both agree at least as well with a theoretical value of 2.0 as the previous single-field versions of this challenge problem. It is noteworthy that the coefficients in the error expressions are higher here than for the single-field error expressions in the previous two challenge problems. This is expected and reflects the manner in which field solver data is transferred and used within the computation kernels of dependent field solvers, e.g. interpolation to Gauss points.

The input files associated with this calculation are in the Aleph repository at
`examples/verification/1d/VT_coupled_oneway_nodes`.

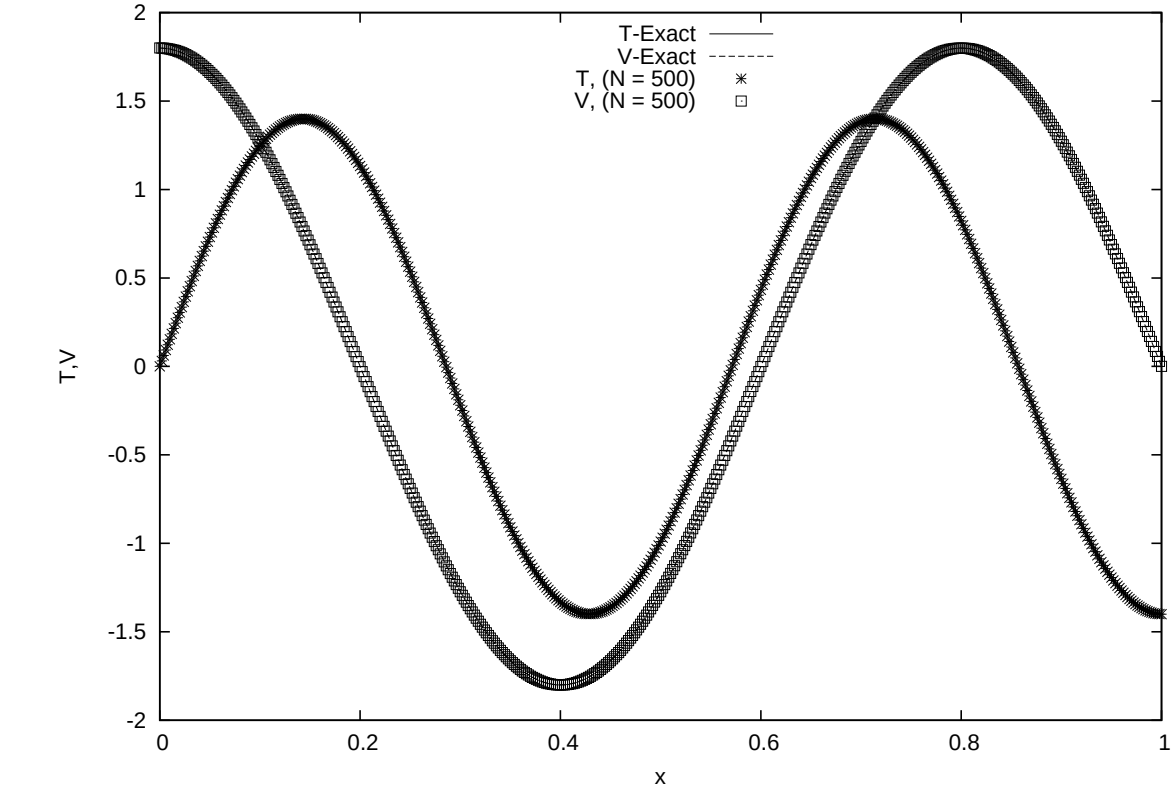

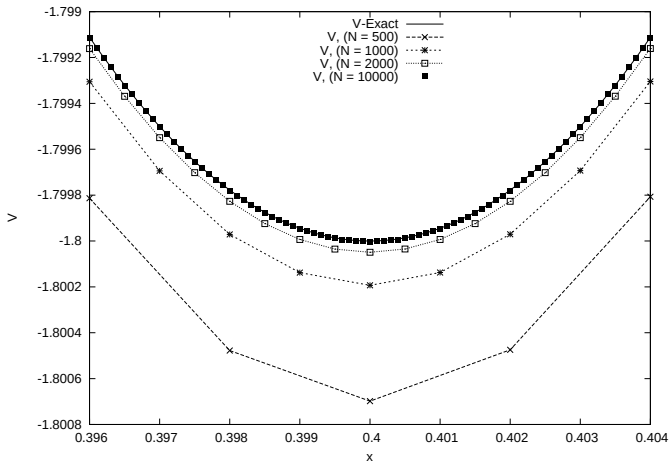

(a) V-field mesh refinement results.

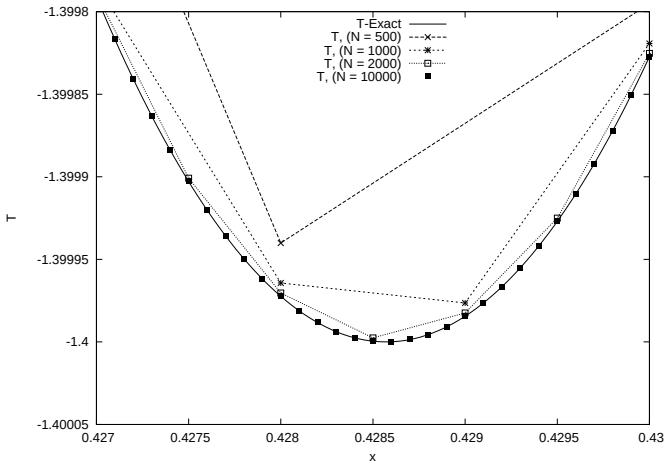

(b) T-field mesh refinement results.

Figure 1.5. Comparison of numerical and exact solutions for various mesh refinement levels for Challenge Problem 4. Mesh spacing Δx is related to number of elements N by $\Delta x = 1.0/N$. The unequal spacing of the errors in the bottom two figures reflects the order of convergence quantified in Figure 1.6.

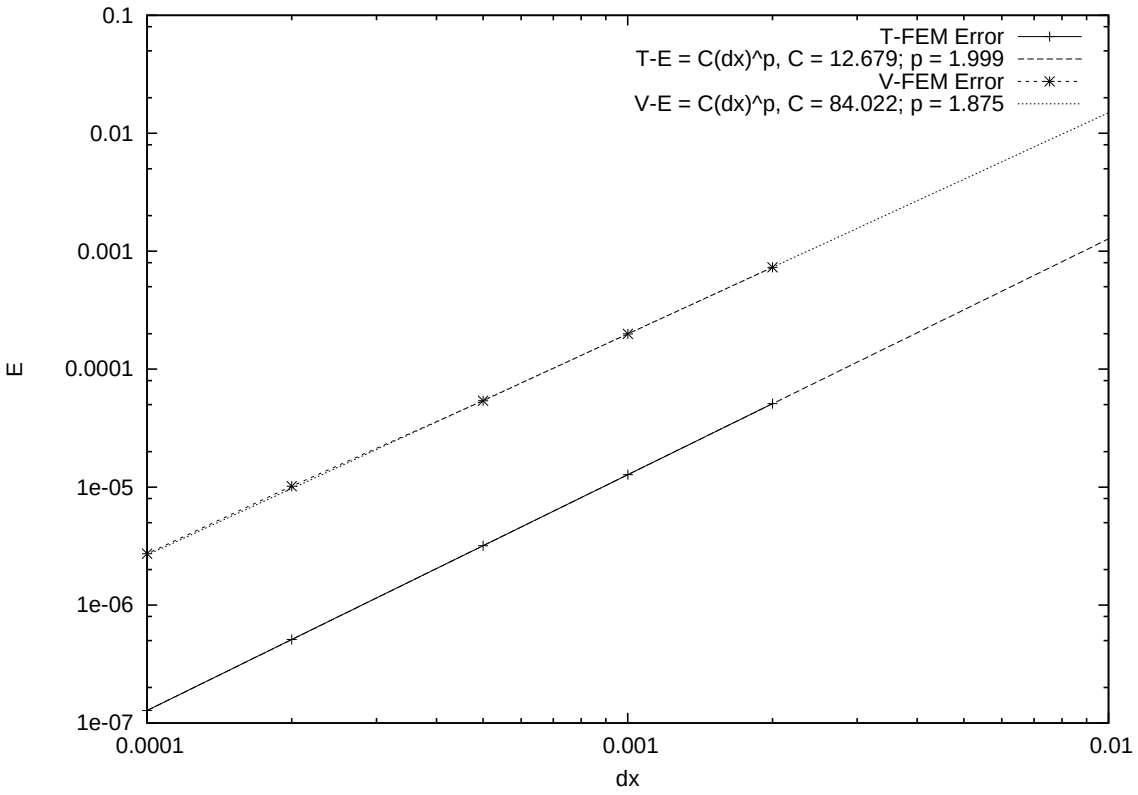

Figure 1.6. Observed order-of-accuracy for Challenge Problem 4. The dashed and dotted lines are least-squares fits to the numerical error.

1.5 Problem 5: Trivial Transient Linear Heat Conduction

This challenge problem introduces time dependence into the thermal conduction model as follows:

$$\rho c_p \frac{\partial T}{\partial t} - k \frac{\partial^2 T}{\partial x^2} = \dot{Q} \tag{1.8}$$

and uses the following initial and boundary conditions:

$$\begin{aligned} \frac{\partial T}{\partial x}(t,0) &= 0 \\ \frac{\partial T}{\partial x}(t,1) &= 0 \\ T(0,x) &= 300.0 \end{aligned} \tag{1.9}$$

The thermal material properties ρ, c_p and k represent density, heat capacity and thermal conductivity and are assigned values of $2.7\text{kg}/\text{m}^3$, $1.2\text{m}^2/(\text{s}^2 \cdot \text{K})$ and $1.0\text{W}/(\text{m} \cdot \text{K})$, respectively. A constant uniform power source is applied as $\dot{Q} = 1000\text{W}/\text{m}^3$.

For time-dependent field solves, Aleph uses an explicit forward Euler method which is accurate to $O(\Delta t)$. The particular boundary conditions for this challenge problem are chosen to produce a spatially constant solution that evolves linearly in time. In the absence of any spatial gradients, Aleph's time integration method should capture this exactly and with no stability restrictions regardless of the size of time steps. To test this, the following time step sizes were used $\Delta t = 0.01, 0.001, 0.0001, 0.00001, 0.000001s$ to run the simulation to $0.02s$. Numerical results were checked to ensure a flat spatial profile and values were compared to the exact solution of $T(0.02, x) = 306.1728395$. Numerical values for all time step sizes agreed perfectly (to the last significant digit) with the exact solution value.

The input files associated with this calculation are in the Aleph repository at
`examples/verification/1d/constant_volumetric_heating_source_term`.

1.6 Problem 6: Transient Linear Heat Conduction

This challenge problem assesses non-trivial time dependence by using the model of eq. (1.8) with $\dot{Q} = 0$ and the following initial and boundary conditions:

$$\begin{aligned} T(t,0) &= 0 \\ T(t,1) &= 0 \\ T(0,x) &= \sin(m\pi x) \end{aligned} \tag{1.10}$$

The density, heat capacity and thermal conductivity were all assigned a value of 1.0, and the adjustable parameter $m = 1.0$. The problem was run for a sequence of time steps consisting of $\Delta t = 0.002, 0.001, 0.0005, 0.0002, 0.0001$ using a mesh of $\Delta x = 0.01$. A comparison of numerical and exact solutions for this problem are shown in Figure 1.7. The amplified region near $x = 0.5$ shows a difference between exact and numerical solutions that appears to vary directly with the time step size Δt. To quantify this, the error of the numerical solutions was computed as $E \equiv ||T(0.02,x) - T_{\Delta t,\Delta x=0.01}(0.02,x)||_2$ using the exact solution $T(t,x) = e^{-\pi^2 t}\sin(\pi x)$. This error is plotted against the time step size in Figure 1.8 along with a best-fit to the assumed functional form for discretization error $E = C(\Delta t)^p$. The observed order-of-accuracy for Aleph's time integrator is $p = 1.02$, which is in good agreement with the expected theoretical value of 1.0.

The input files associated with this calculation are in the Aleph repository at `examples/verification/1d/trans_T_dirichlet`.

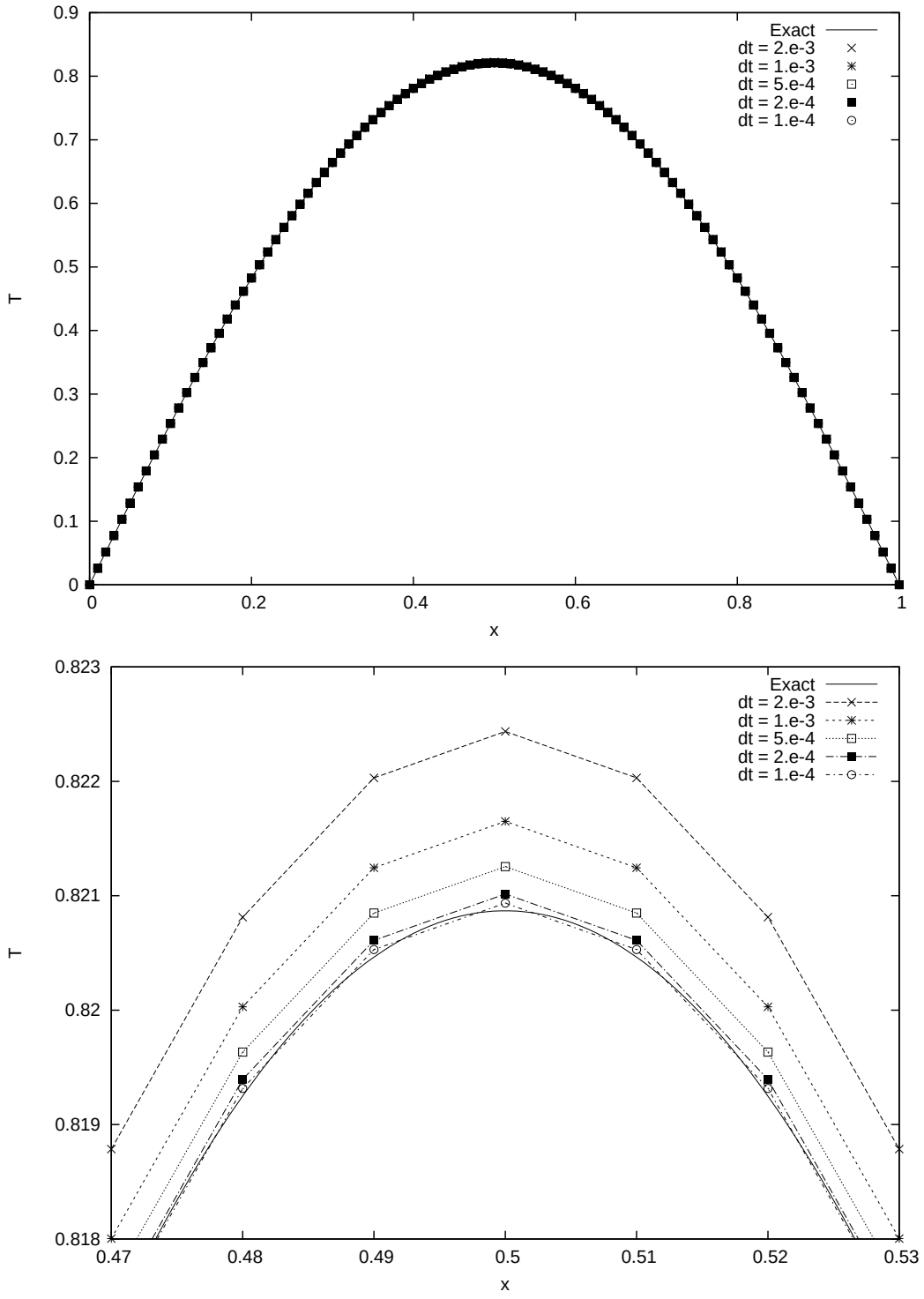

Figure 1.7. Comparison of numerical and exact solutions for various mesh refinement levels for Challenge Problem 6 at $t = 0.02$. The bottom plot shows the difference between exact and numerical solutions to vary directly with the time step size Δt, and this is quantified in Figure 1.8.

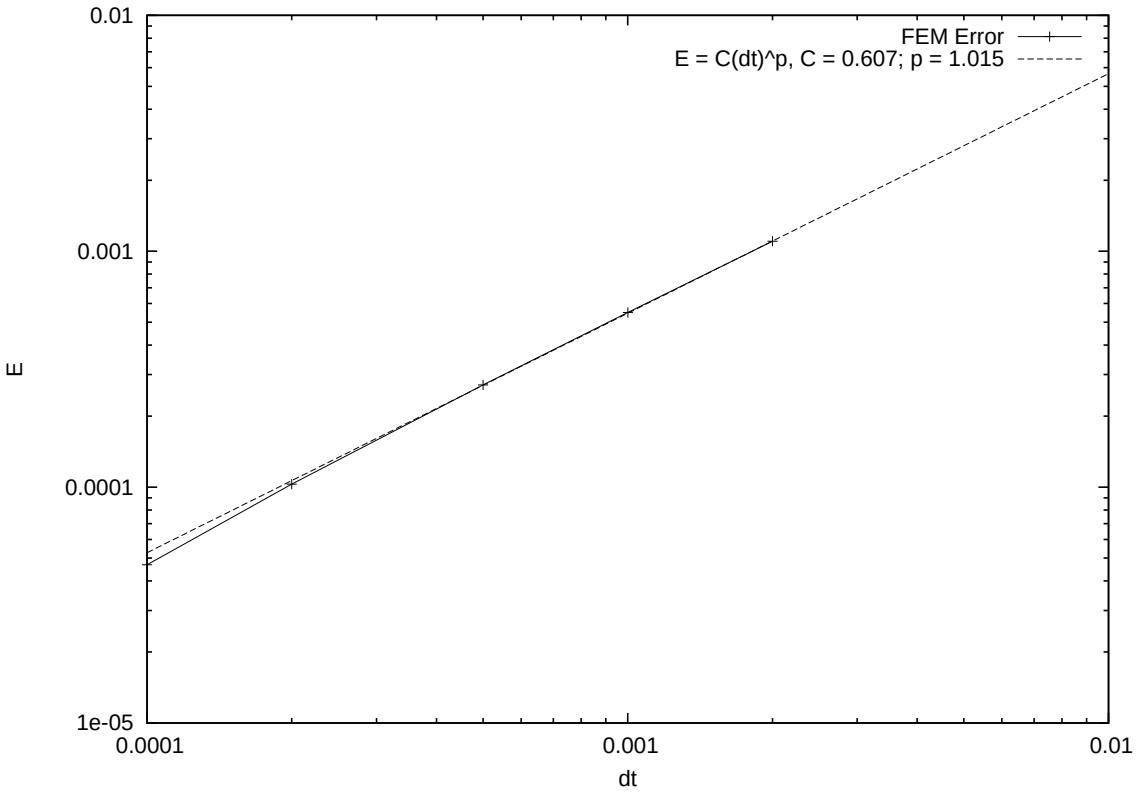

Figure 1.8. Observed order-of-accuracy for Challenge Problem 6. The dashed line is a least-squares fit to the numerical error.

1.7 Problem 7: Transient Thermal Flux Boundary Condition

This challenge problem is the same as Problem 6 but with the $x = 1$ boundary condition replaced by a Neumann condition that admits the same analytic solution, i.e. $T(t,x) = e^{-\pi^2 m^2 t}\sin(m\pi x)$. Again using $m = 1.0$ leads to the following boundary and initial conditions

$$T(t,0) = 0 \tag{1.11}$$

$$\frac{\partial T}{\partial x}(t,1) = -\pi e^{-\pi^2 t} \tag{1.12}$$

$$T(0,x) = \sin(\pi x) \tag{1.13}$$

The importance of this problem lies in demonstrating Aleph's ability to treat time-dependent Neumann boundary conditions. The numerical and exact solutions are shown in Figure 1.9, and the error is plotted against the time step size in Figure 1.10 along with a best-fit to the assumed functional form for discretization error $E = C(\Delta t)^p$. The solutions are nearly indistinguishable from those in Problem 6 as they should be. The observed order-of-accuracy is $p = 0.99$, which is in good agreement with the expected theoretical value of 1.0.

The input files associated with this calculation are in the Aleph repository at `examples/verification/1d/trans_T_neumann`.

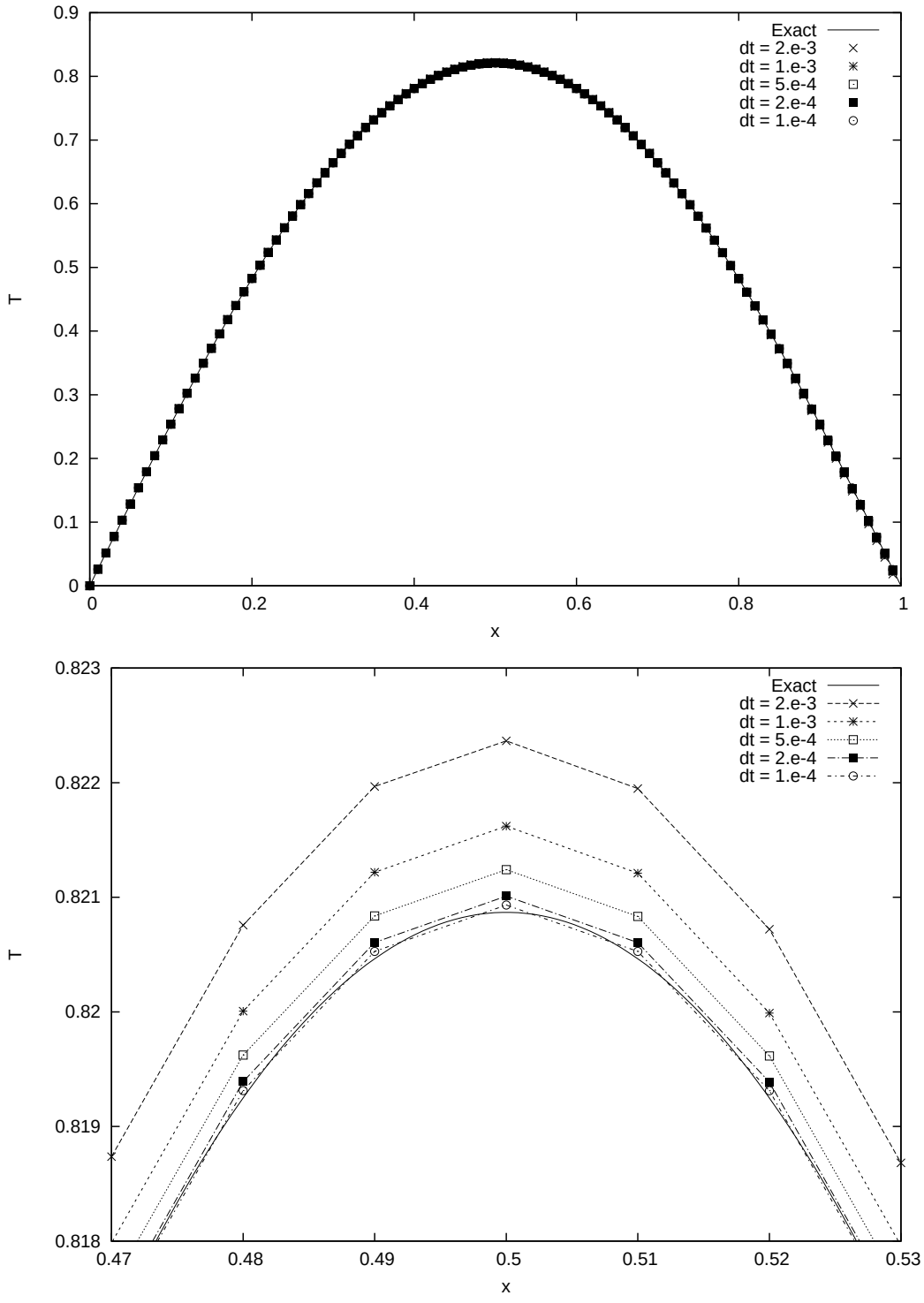

Figure 1.9. Comparison of numerical and exact solutions for various mesh refinement levels for Challenge Problem 7 at $t = 0.02$. The bottom plot shows the difference between exact and numerical solutions to vary directly with the time step size Δt, and this is quantified in Figure 1.10.

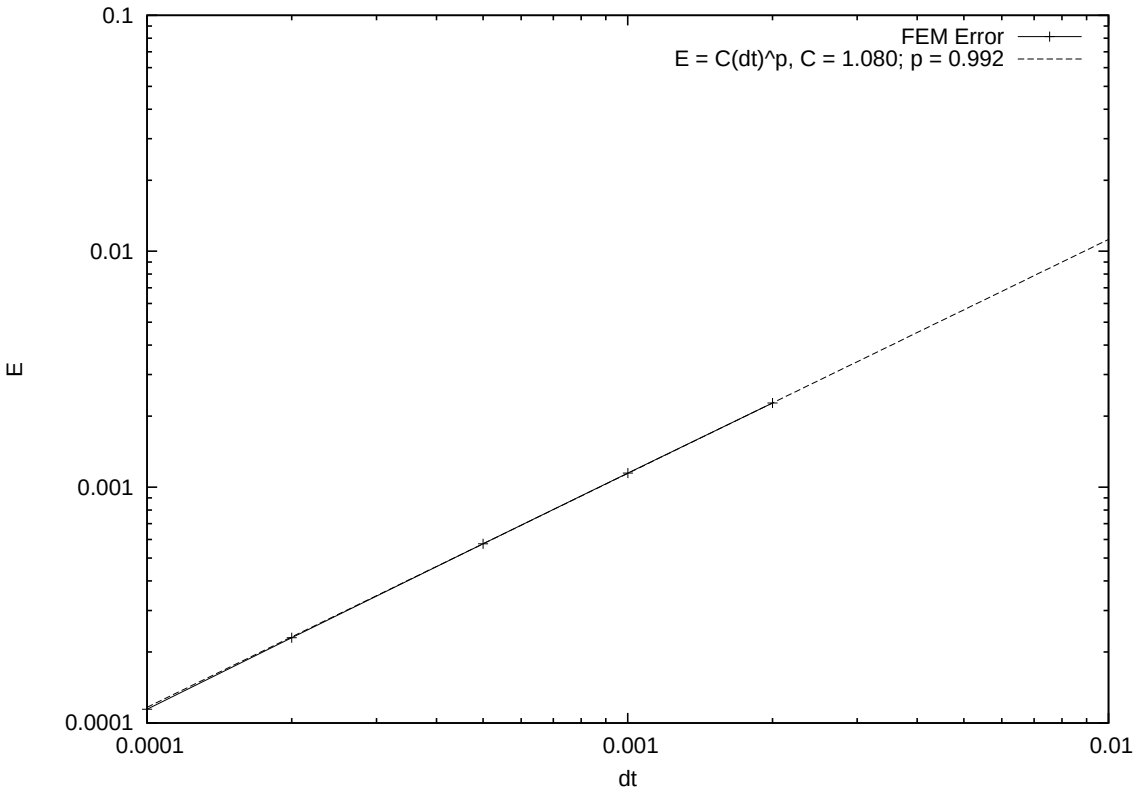

Figure 1.10. Observed order-of-accuracy for Challenge Problem 7. The dashed line is a least-squares fit to the numerical error.

1.8 Problem 8: Semi-Infinite Conduction with Constant Surface Heat Flux

This challenge problem is intended to provide a more physical example than the previous problems. Physically meaningful values and SI units are used to model heat conduction into a semi-infinite slab heated on one side by a constant thermal heat flux. Model parameters are summarized in Table 1.1.

Parameter	Value & Units	Description
ρ	$2.7\ \mathrm{kg/m^3}$	density
k	$0.4\ \mathrm{W/(m \cdot K)}$	thermal conductivity
c_p	$1.2\ \mathrm{m^2/(s^2 \cdot K)}$	heat capacity
T_i	300 K	initial temperature
q_s	$5.0 \times 10^4\ \mathrm{W/m^2}$	surface heat flux
α	$k/(\rho \cdot c_p) = 0.123\ \mathrm{m^2/s}$	thermal diffusivity

Table 1.1. Parameters used in Challenge Problem 8.

This problem has the following analytic solution:

$$T(t,x) = T_i + \frac{2q_s\sqrt{\frac{\alpha t}{\pi}}}{k}\exp\left(\frac{-x^2}{4\alpha t}\right) - \frac{q_s x}{k}\mathrm{erfc}\left(\frac{x}{2\sqrt{\alpha t}}\right) \tag{1.14}$$

This problem represents a well-studied physically meaningful problem [3] and is a departure from previous challenge problems which contrive analytic solutions and assume simplistic material property values. Figures 1.11 and 1.12 show relatively coarse (in Δx and Δt) Aleph solutions compared to the exact solution over space and time, respectively. While these results appear good, rigorous code verification must rely on more quantitative underpinnings. Accordingly, we present the order-of-convergence behavior in Figure 1.13 for time step size and in Figure 1.14 for mesh size. Using $\Delta x = 0.002$ m the observed order-of-accuracy for Δt convergence is $p_{\Delta t} = 0.975$. Using $\Delta t = 2.0 \times 10^{-5}$ s, the Δx convergence is $p_{\Delta x} = 2.06$. These convergence rates compare favorably with the expected theoretical values of 1.0 and 2.0, respectively.

The input files associated with this calculation are in the Aleph repository at `examples/verification/1d/trans_T_neumann_particles_with_SI_units`.

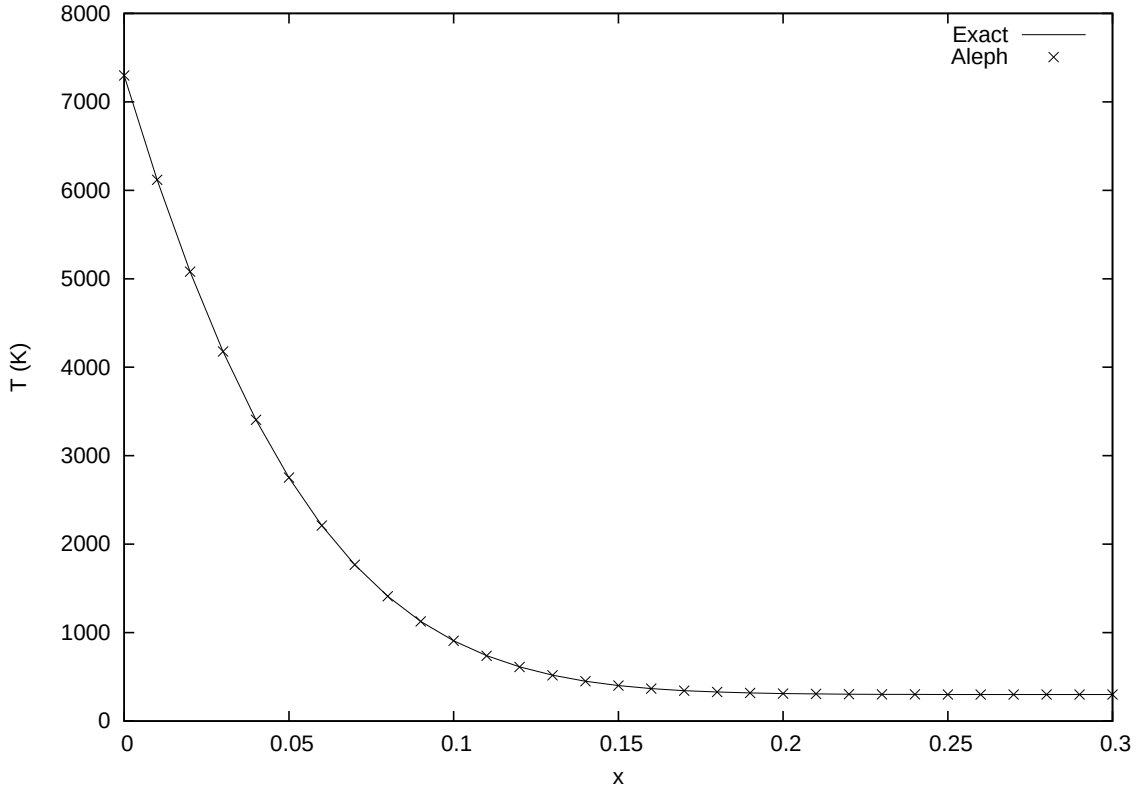

Figure 1.11. $T(0.02,x)$ using mesh $\Delta x = 0.01$ m and timestep $\Delta t = 0.0001$ s for Challenge Problem 8.

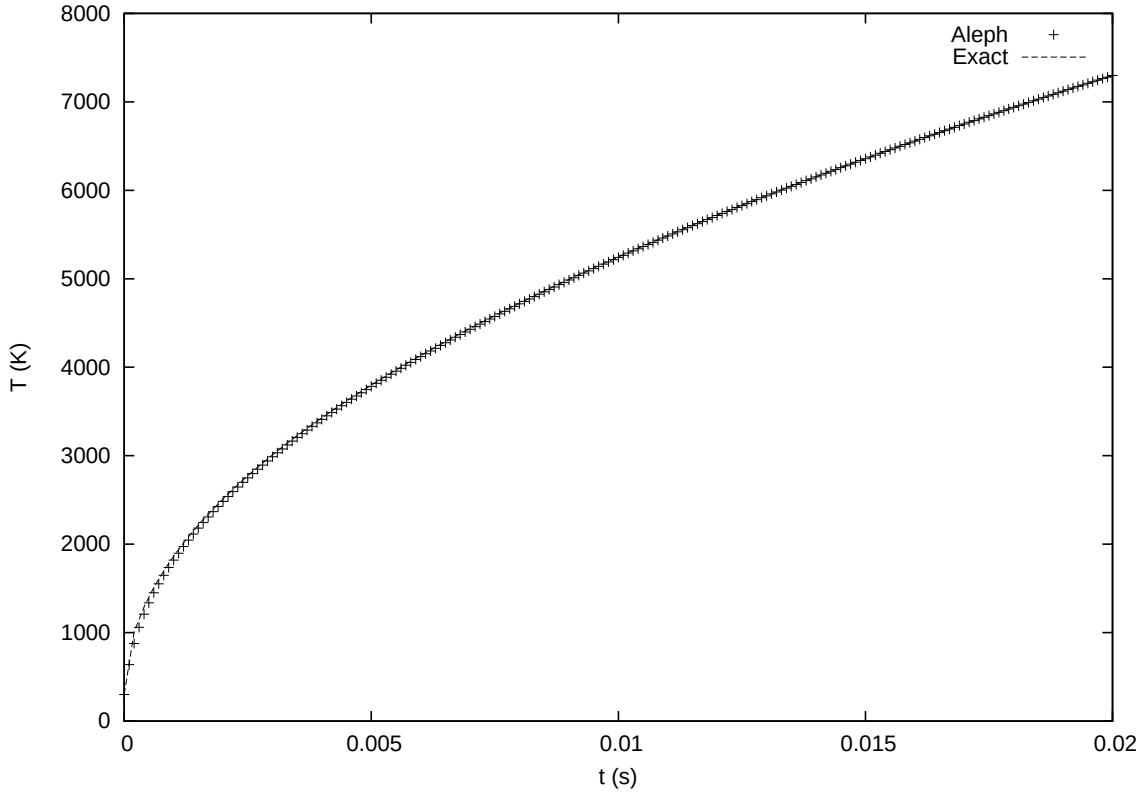

Figure 1.12. $T(t,0)$ using mesh $\Delta x = 0.01$ m and timestep $\Delta t = 0.0001$ s for Challenge Problem 8.

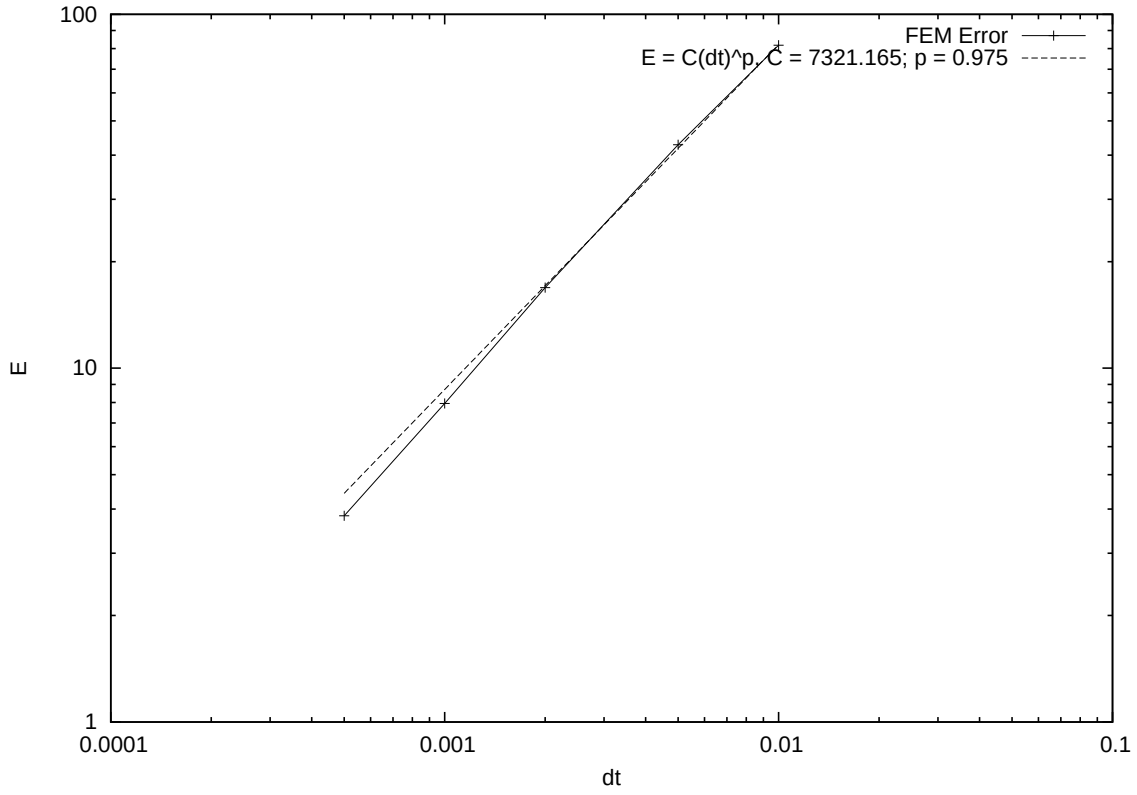

Figure 1.13. Observed order-of-accuracy for Δt using $\Delta x = 0.002$ m for Challenge Problem 8. The dashed line is a least-squares fit to the numerical error.

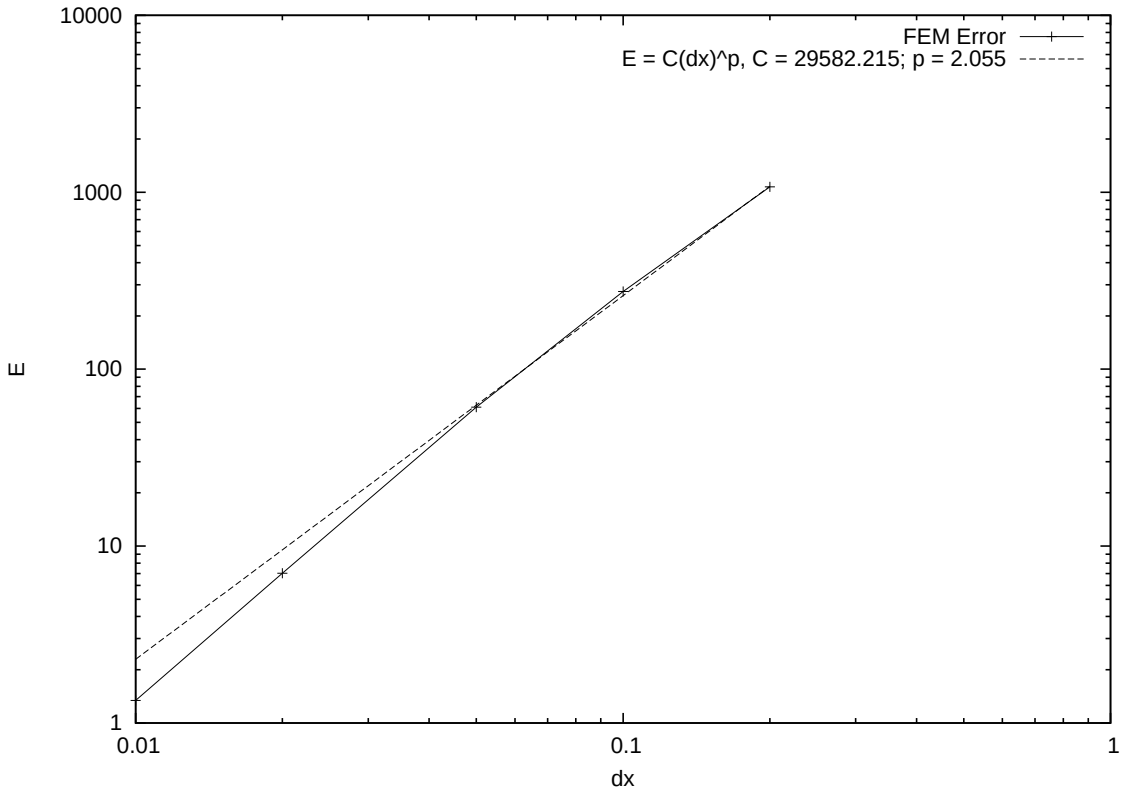

Figure 1.14. Observed order-of-accuracy for Δx using $\Delta t = 2.0 \times 10^{-5}$ s for Challenge Problem 8. The dashed line is a least-squares fit to the numerical error.

1.9 Problem 9: Combined Particle-Driven and Heatloss Transient Thermal Flux Boundary Conditions

This challenge problem incorporates SI units along with models for both surface heating due to impacting particles and surface cooling due to thermal particle emission to produce numerically equivalent time-dependent thermal flux behavior to problem 7. In addition, the ability of Aleph to correctly treat multiple impacting particle types is tested by creating two different types of particles. A predetermined flux of both types is injected into a domain next to the thermal conduction region. Particle velocities are specified as a function of time such that the kinetic energy imparted at impact with the thermal domain is numerically twice that of eq. (1.12). This source of thermal flux is then offset by a heatloss three times the value of eq. (1.12) by activating a thermal emission model in Aleph based on the Antoine equation. The Antoine coefficients are chosen to be functions of time to produce a net thermal flux numerically equivalent to eq. (1.12).

To derive the expressions for the two competing thermal fluxes, we recall eq. (1.8) and express the case for no thermal source, $\dot{Q} = 0$ as

$$\frac{\partial T}{\partial t} - \alpha \frac{\partial^2 T}{\partial x^2} = 0 \tag{1.15}$$

where $\alpha = k/(\rho C_p) = 1.0\ \mathrm{m}^2/\mathrm{s}$. Because we seek an exact solution comparable to that for problem 7 but now driven by competing thermal flux physical models, we recast the boundary and initial conditions of problem 7 into the following form:

$$\begin{aligned} T(t,-1) &= 0 \\ \frac{\partial T}{\partial x}(t,0) &= -\frac{\pi T_0}{L} \mathrm{e}^{-(\pi/\mathrm{L})^2 \alpha \mathrm{t}} \\ T(0,x) &= T_0 \left(1 + \sin\left(\frac{\pi(x+1)}{L}\right) \right) \end{aligned} \tag{1.16}$$

where $L = 1.0$ (m) is the size of the 1D thermal domain which has been shifted left by 1.0 compared to problem 7, and $T_0 = 1.0$ (K) is chosen as the initial temperature. Together, these parameter values produce the same temperature solution as in problem 7 with the only difference being a temperature shift of 1.0 (K). The shift is required for this problem to allow admissible temperatures to be used with the Antoine equation, i.e., $T > 0$. As defined, this challenge problem admits the exact solution

$$T(t,x) = T_0 \left[1 + \mathrm{e}^{-(\pi/L)^2 \alpha t} \sin\left(\frac{\pi(x+1)}{L} \right) \right], \; x \in [-1, 0] \tag{1.17}$$

which has units of K and reduces to the shifted exact solution of problem 7 for the chosen values of T_0, L and α. The corresponding temperature gradient at the boundary between the thermal and plasma domains is given by:

$$\frac{\partial T}{\partial x}(t,0) = -\frac{\pi T_0}{L} \mathrm{e}^{-(\pi/\mathrm{L})^2 \alpha \mathrm{t}} \tag{1.18}$$

which has units of K/m and reduces to the expression in eq. (1.12) for our chosen parameter values.

To derive the source of thermal flux due to impacting particles, we express the thermal flux into the thermal domain based on the kinetic energy of the impacting particles. For a collection of n particles having mass m (kg) and velocity magnitude v (m/s) impacting a surface of area S (m^2) over an increment of time Δt (s), the magnitude of thermal flux q_p is expressed as

$$q_p = n\frac{mv^2}{2S\Delta t} \tag{1.19}$$

and has units of W/m^2. This quantity is related to the Neumann boundary condition in eq. (1.18) as follows:

$$\mathbf{n}\cdot\mathbf{q} = \mathbf{e}_x \cdot \left(-k\frac{\partial T}{\partial x}\mathbf{e}_x\right) = q_p \tag{1.20}$$

in which the impacting particles provide a source of energy at the boundary. From this equation, the time-dependent particle velocity magnitude (m/s) is given by,

$$v = \sqrt{\frac{2\pi SkT_0\Delta t}{nmL}}\mathrm{e}^{-\frac{1}{2}(\pi/L)^2\alpha t} \tag{1.21}$$

So long as all particles traverse the plasma domain in a single time step, n injected particles with mass m and velocity given by eq. (1.21) would produce the exact magnitude Neumann boundary condition of eq. (1.12). We enforce this condition by choosing L_p such that $v\Delta t \gg L_p$ where L_p is the length of the plasma domain. This effectively enforces deterministic particle behavior in order to accurately assess order-of-convergence.

An opposing heat flux associated with thermal particle emission is specified using the Antoine equation which expresses the vapor pressure P_V as follows [1],

$$\log_{10}(P_V) = A + \frac{B}{T} + C\log_{10}(T) + \frac{D}{T^3} \tag{1.22}$$

This vapor pressure corresponds to a mass flux with magnitude ϕ_e given by

$$\phi_e = \frac{P_V f_c}{\sqrt{2\pi m k_B T}} \tag{1.23}$$

where k_B is Boltzmann's constant [m^2-kg/(s^2-K)], and f_c is a pressure conversion factor needed for ϕ_e to have units of kg/(m^2-s). The mass flux is then converted to a thermal flux of magnitude q_e (W/m^2) using the heat of vaporization H_v (J/kg) as follows:

$$q_e = (H_v + 2k_B T)\,\phi_e \tag{1.24}$$

We can relate this equation to eq. (1.18) as follows:

$$\mathbf{n}\cdot\mathbf{q} = \mathbf{e}_x \cdot \left(-k\frac{\partial T}{\partial x}\mathbf{e}_x\right) = q_e \tag{1.25}$$

If we assign Antoine coefficients $B = C = D = 0$, we can then solve for the Antoine coefficient A needed to produce a heat flux equal in magnitude to that of eqs. (1.12) and (1.20). We also use the

fact that $T(t,0) = T_0$ for this challenge problem. Together, these result in the following expression for A,

$$A = \log_{10}\left[\left(\frac{k\pi T_0\sqrt{2\pi m k_B T_0}}{(H_v + 2k_B T_0)\, f_c L}\right) \mathrm{e}^{-(\pi/L)^2 \alpha t}\right] \tag{1.26}$$

The importance of this challenge problem lies in demonstrating Aleph's ability to treat aggregate, time-dependent Neumann boundary conditions involving particle-based events, e.g., thermal absorption and emission. Accordingly, we construct a net thermal heat flux numerically equivalent to eq. (1.12) by imposing a thermal flux driven by two different particle types having the same mass and number and both types injected with velocity specified using eq. (1.21). This incoming heat flux is offset by using eq. (1.24). The final form of the boundary condition for this challenge problem represents a net time-dependent, particle-based Neumann boundary condition equal in magnitude and direction to eq. (1.12) and is expressed as

$$\mathbf{n}\cdot\mathbf{q} = \mathbf{e}_x \cdot \left(-k\frac{\partial T}{\partial x}\mathbf{e}_x\right)\Bigg|_{x=0} = 2q_p - 3q_e \tag{1.27}$$

Figure 1.15 shows the exact and numerical solutions which are nearly indistinguishable from those for problems 6 and 7 except for the vertical shift of 1.0 in T and the shift of the domain from $[0,1]$ to $[-1,0]$. The vertical shift is needed to avoid zero values of T for which the logarithm is undefined, and the shift of the domain reflects particles injected from the right at $x = 1$ and impacting the thermal domain surface at $x = 0$. Figure 1.16 shows the error plotted against the time step size along with a best-fit to the assumed functional form for discretization error using a mesh with $\Delta x = 0.01$. The observed order-of-accuracy for Aleph's time integrator is $p = 1.11$, which is in good agreement with the expected theoretical value of 1.0.

The input files associated with this calculation are in the Aleph repository at `examples/verification/1d/trans_T_neumann_multi_flux`.

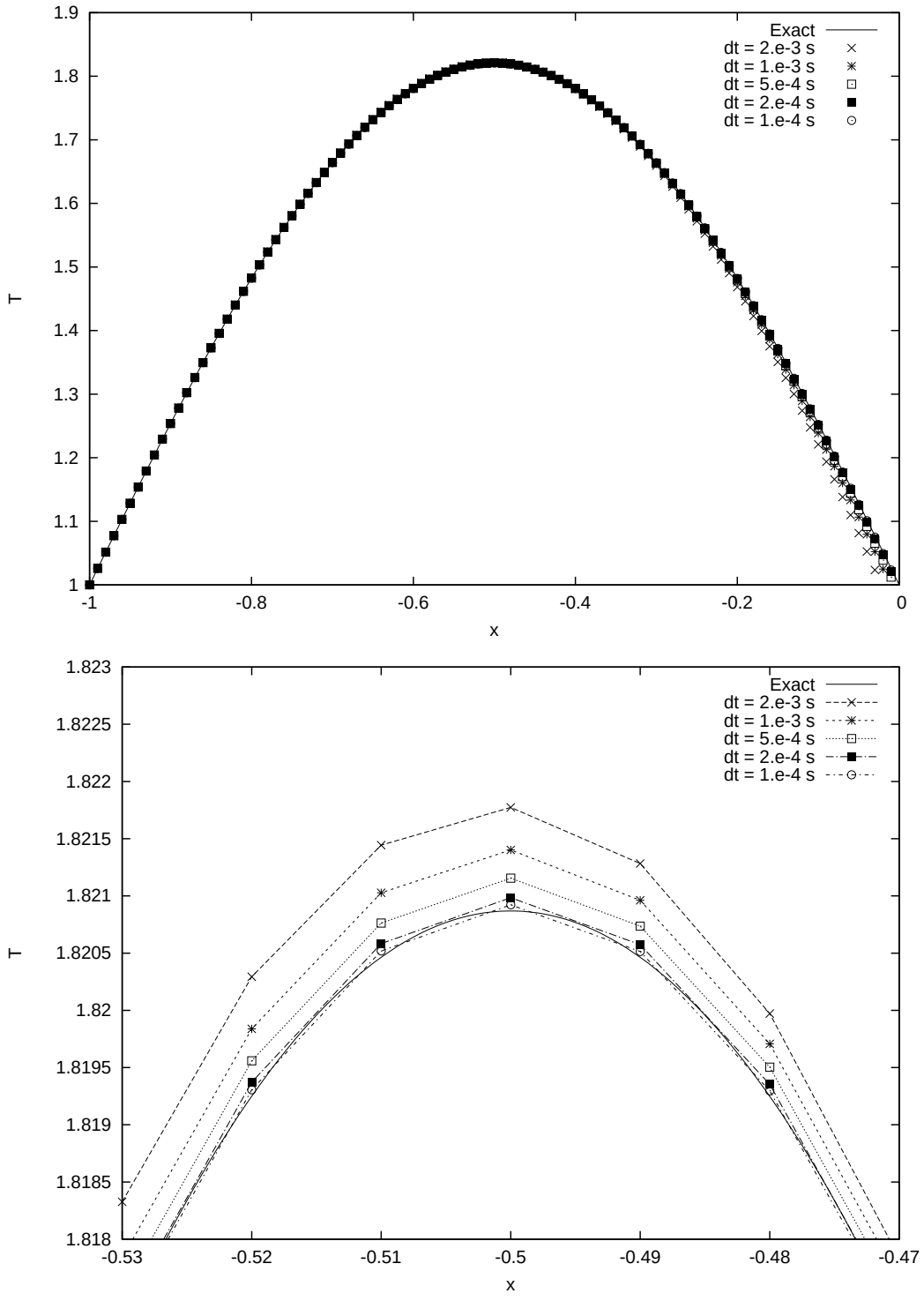

Figure 1.15. Comparison of numerical and exact solutions for various mesh refinement levels for Challenge Problem 9 at $t = 0.02$ s. The bottom plot shows the difference between exact and numerical solutions to vary directly with the time step size Δt (s), and this is quantified in Figure 1.16.

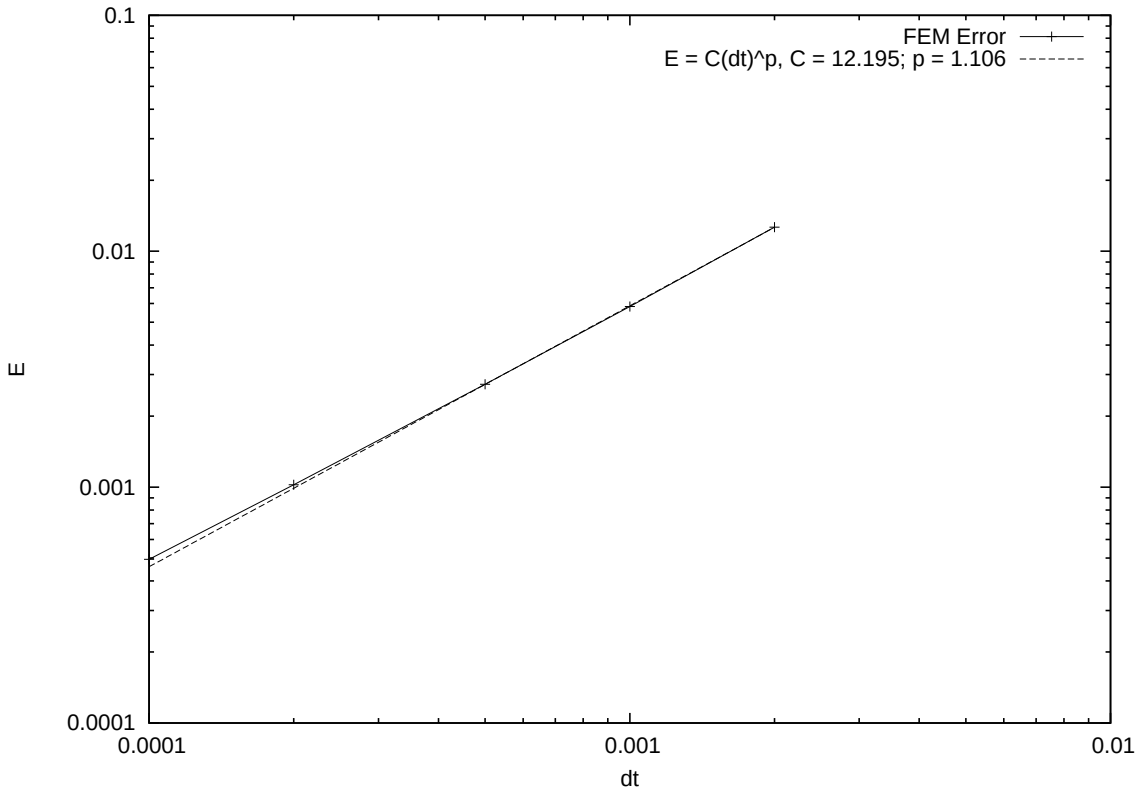

Figure 1.16. Observed order-of-accuracy using $\Delta x = 0.01$ (m) for Challenge Problem 9. The dashed line is a least-squares fit to the numerical error.

Chapter 2

2D & 3D Verification

This chapter extends the previous collection of challenge problems to higher spatial dimensions. These challenge problems exercise different parts of the Aleph code than that exercised for 1D problems because 1D meshes are not natively supported by the Exodus library used by Aleph. Both 2D and 3D meshes are natively supported by the Exodus library, and the code is the same for both. Therefore, we have very high confidence that code verified for either a 2D or 3D problem preserves correct behavior for both.

2.1 Problem 10: 2D Steady Linear Heat Conduction with Source

The first departure from 1D is a 2D analogue of Challenge Problem 2. The governing model equation is now expressed more generally, and the source term is constructed to test the variation of the solution in both spatial dimensions. This is expressed as follows:

$$\nabla^2 T = m\pi^2(n^2+l^2)\sin(n\pi x)\sin(l\pi y) \tag{2.1}$$

with compatible boundary conditions

$$\begin{aligned} T(0,y) &= 0 \\ T(1,y) &= m\sin(n\pi)\sin(l\pi y) \\ T(x,0) &= 0 \\ T(x,1) &= m\sin(n\pi x)\sin(l\pi) \end{aligned}$$

For this verification study, parameter values of $m = 1.4$, $n = 0.5$ and $l = 2.0$ were chosen to produce different solution structure in the x and y-directions. This steady 2D problem admits the exact solution $T(x) = m\sin(n\pi x)\sin(l\pi y)$, and the FEM solution for the coarsest mesh considered is shown in Figure 2.2. Exact and numerical solutions are shown in Figure 2.3 along the line $x = 0.5$. Note that the x-values plotted correspond to an equally-spaced interpolation of the numerical solutions along the y-direction at $x = 0.5$ performed using the Ensight visualization software package version 9.2.1(c). For assessing numerical error, the same measure is used as before, i.e., $E \equiv ||T(x,y) - T_{\Delta x,\Delta y}(x,y)||_2$, and a sequence of meshes characterized by

$\Delta x = \Delta y = 0.02, 0.01, 0.005, 0.002$. The order-of-convergence was determined via a fit to the assumed functional form for discretization error $E = C(h)^p$ where h is a representative mesh size based on Δx and Δy. The coarsest mesh is shown in Figure 2.1. For this problem, $h = \Delta x = \Delta y$. The FEM error along with the best fit are shown in Figure 2.4. For this challenge problem,

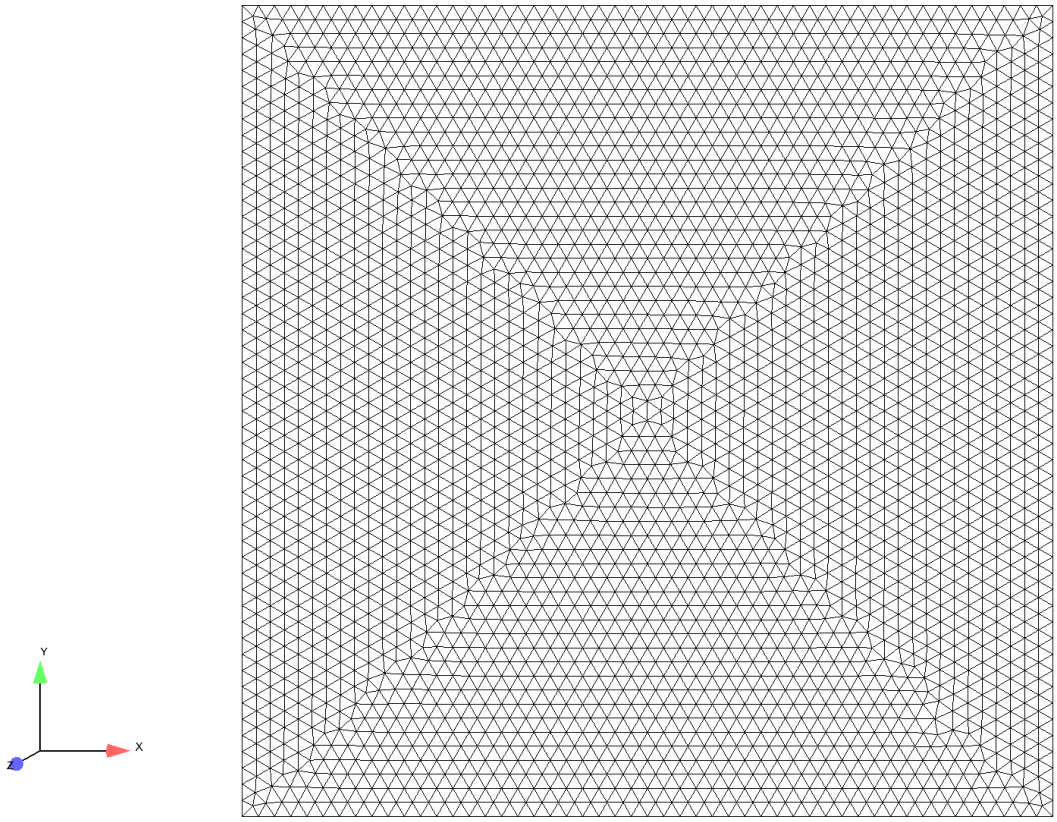

Figure 2.1. Coarsest 2D mesh of unit square with origin at lower-left and $\Delta x = \Delta y = 0.02$.

Aleph's FEM field solver exhibits an order-of-accuracy of 2.000, in exact agreement with the theoretical value.

The input files associated with this calculation are in the Aleph repository at `examples/verification/2d/T_only`.

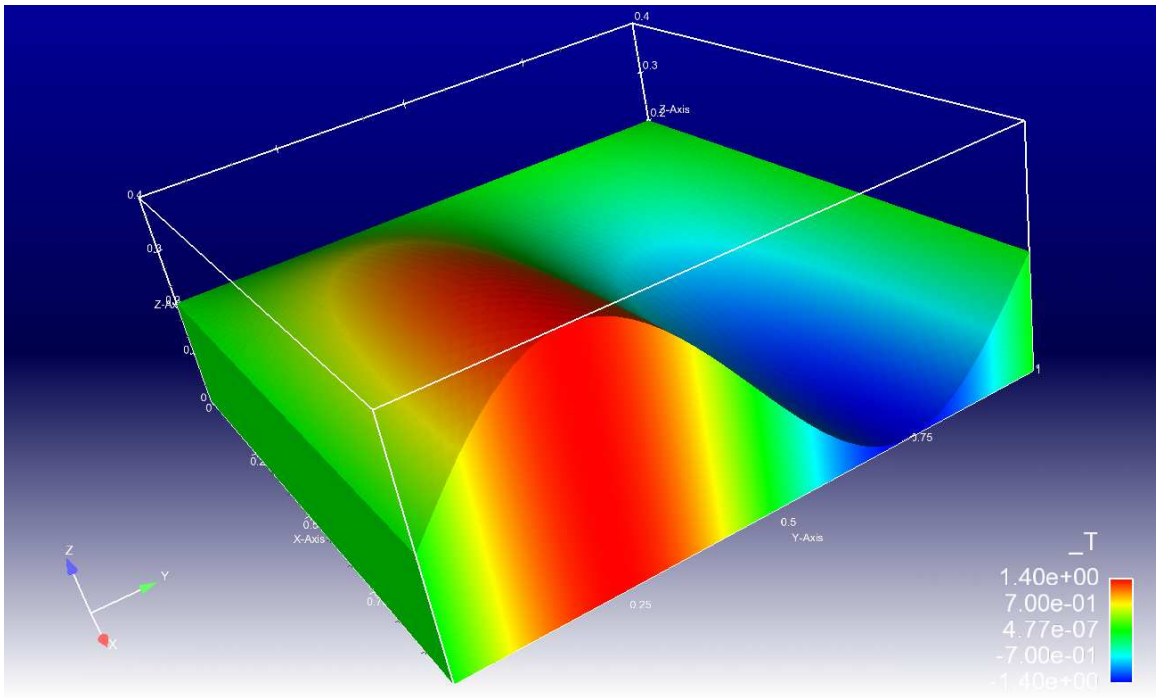

Figure 2.2. FEM solution on coarse mesh for Challenge Problem 10.

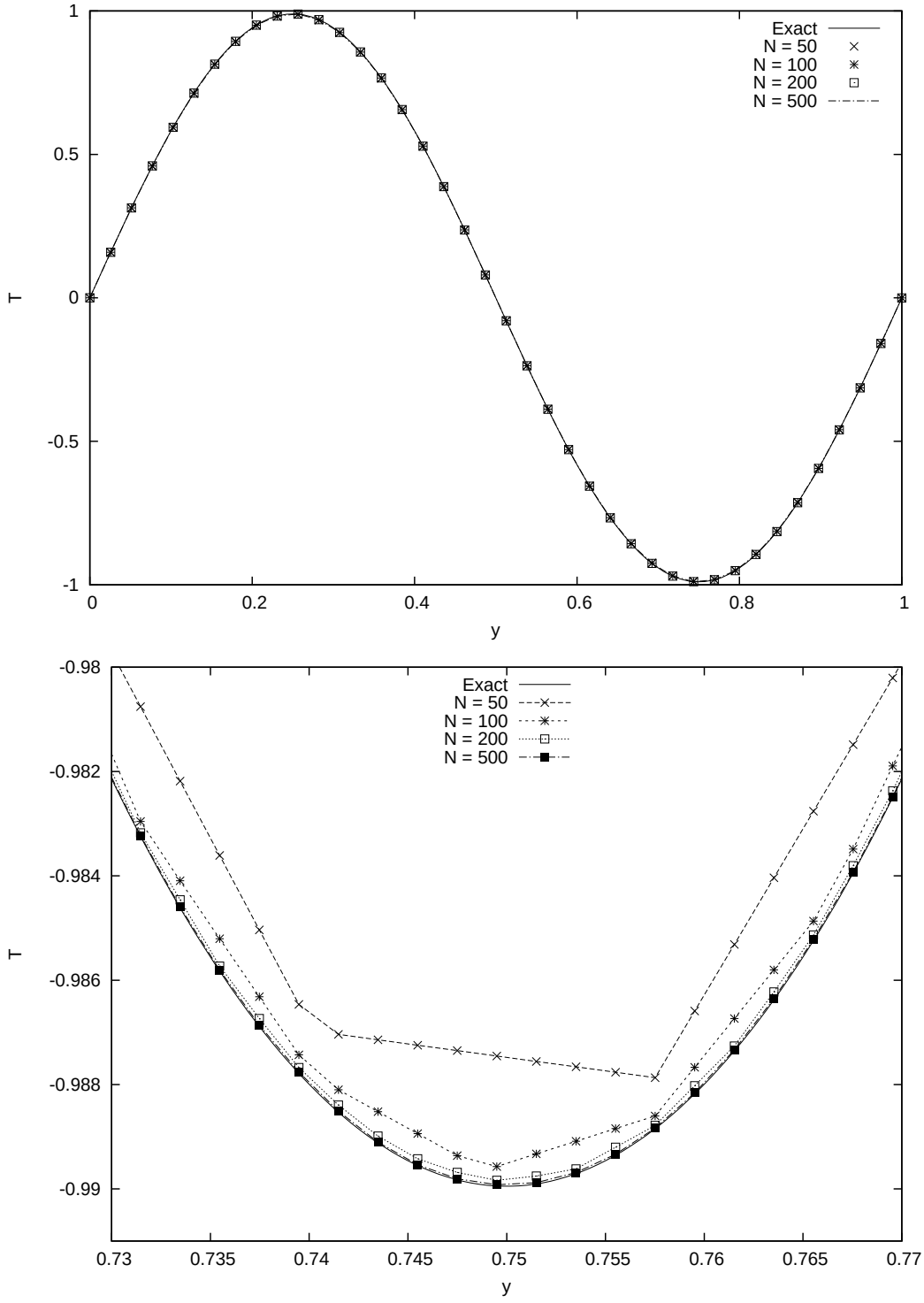

Figure 2.3. Comparison of numerical and exact solutions for various mesh refinement levels for Challenge Problem 10. Plotted x-values correspond to an equally-spaced interpolation of the numerical solutions along the y-direction at $x = 0.5$ using 40 interpolation points (top) and 500 interpolation points (bottom).

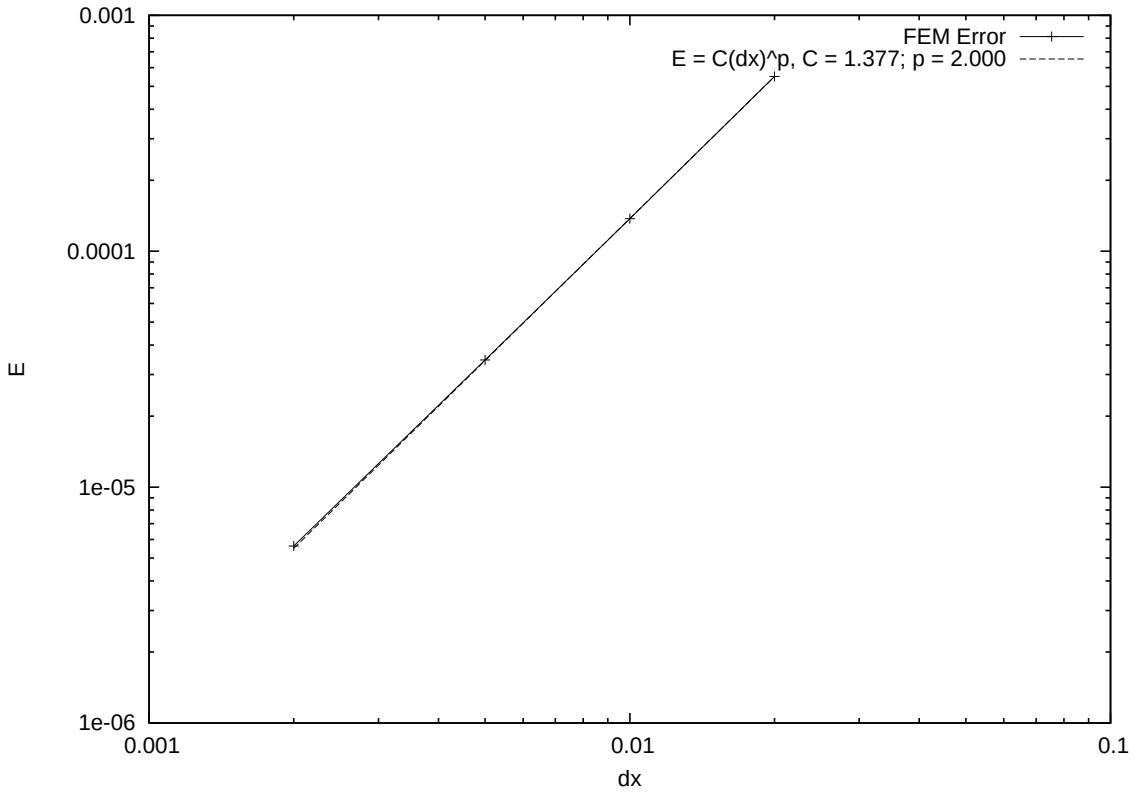

Figure 2.4. Observed order-of-accuracy for Challenge Problem 10. The dashed line is a least-squares fit to the numerical error.

2.2 Problem 11: 3D Steady & Parallel Transient Linear Heat Conduction

This challenge problem extends the previous problem to time-dependent 3D and exercises the parallel algorithm features of Aleph's FEM solver. The problem is constructed to produce an analytic solution with spatial structure that varies in each of the three dimensions. The problem definition is as follows,

$$\rho c_p \frac{\partial T}{\partial t} - k\nabla^2 T = 0 \tag{2.2}$$

with compatible initial and boundary conditions as

$$\begin{aligned}
T(t,0,y,z) &= 0 \\
T(t,1,y,z) &= 0 \\
T(t,x,0,z) &= 0 \\
T(t,x,1,z) &= 0 \\
T(t,x,y,0) &= 0 \\
T(t,x,y,1) &= 0 \\
T(0,x,y,z) &= \sin(n\pi x)\sin(l\pi y)\sin(k\pi z)
\end{aligned}$$

where ρ, c_p and k are all assigned values of 1.0; and n, l and k are 1, 2 and 3, respectively. On a spatial domain consisting of a unit cube, this choice of parameters admits the homogeneous Dirichlet boundary conditions. The exact solution used to assess numerical errors is $T(x) = e^{-\pi^2 t(n^2+l^2+k^2)}\sin(n\pi x)\sin(l\pi y)\sin(k\pi z)$. Unstructured tetrahedral meshes characterized by $h = \Delta x = \Delta y = \Delta z = 0.2, 0.1, 0.05, 0.033$ and 0.025 are used with a fixed time step of $\Delta t = 2.0 \times 10^{-5}$ to assess spatial order-of-convergence. Representative numerical solutions on the finest 3D mesh are shown in Figure 2.5. A comparison of the exact and numerical solutions for the different Δx are shown in Figure 2.6 where the parameter s is the distance along the line from $(x,y,z) = (0,0,0)$ to $(1,1,1)$. Interpolations were performed using the Ensight visualization software package version 9.2.1(c). Temporal order-of-convergence is determined using $\Delta t = 0.01, 0.005, 0.002, 0.001, 0.0005$ on the mesh characterized by $h = 0.033$. A comparison of the exact and numerical solutions for the different Δt are shown in Figure 2.7 where s is the same. Numerical errors are plotted along with the best-fit curves for temporal and spatial orders-of-convergence in Figures 2.8 and 2.9, respectively. The spatial order-of-convergence was found to be 1.73 for the problem with $n = 1$, $l = 2$ and $k = 3$. The deviation from the theoretical value of 2.0 was suspected to be due to the degree of solution curvature, particularly in the z-direction. Accordingly, another order-of-convergence study was performed using $n = l = k = 1$ and is included in Figure 2.9. This easier version of the problem exhibits improved order-of-convergence, even above the theoretical value which is not uncommon for mesh convergence studies of transient problems.

A test of Aleph's parallel solve capability is implicit in the temporal convergence study in which each run was performed on 4 cores on a previously decomposed mesh with $h = 0.033$.

For this challenge problem, Aleph's FEM field solver exhibits temporal order-of-accuracy of $p_{\Delta t} = 0.98$ and spatial order-of-accuracy $p_{\Delta x} = 1.73$.

The input files associated with this calculation are in the Aleph repository at `examples/verification/3d/trans_T_dirichlet`.

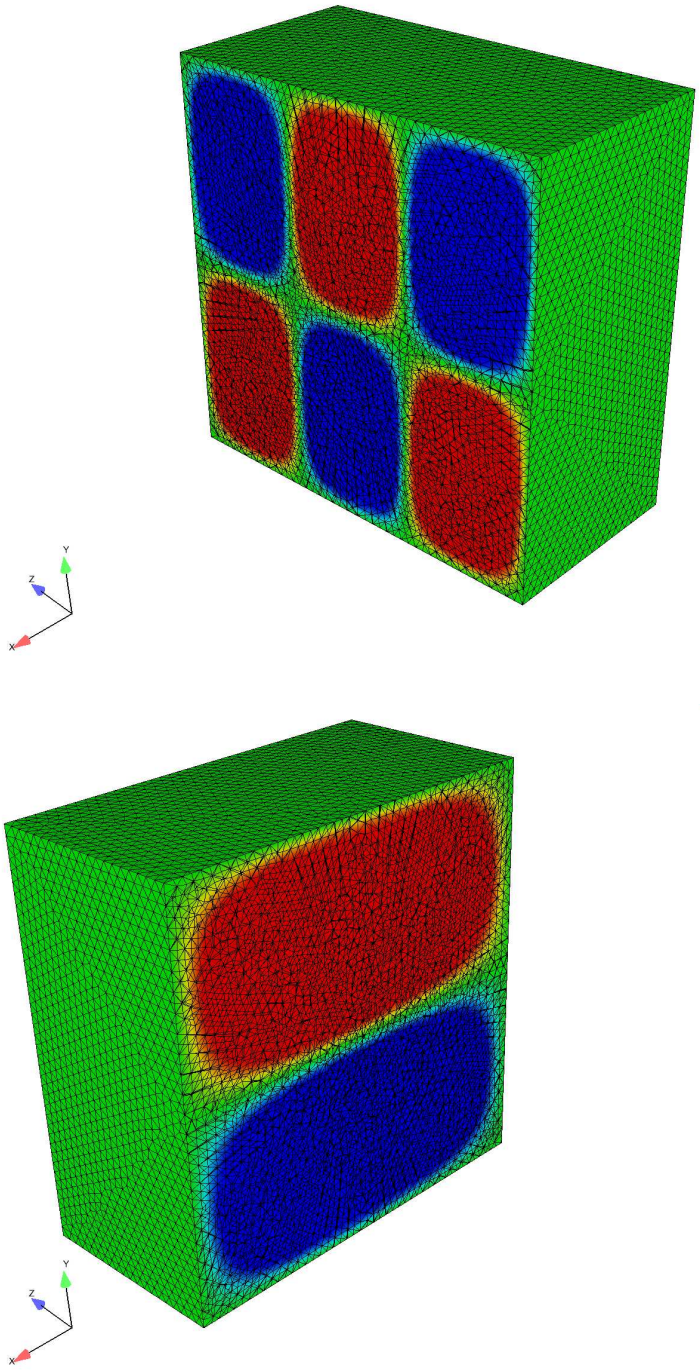

Figure 2.5. FEM solution on fine mesh at $t = 0.00838$ for Challenge Problem 11 at $t = 0.02$. The mesh has been clipped with planes at $x = 0.5$ (top) and $z = 0.5$ (bottom).

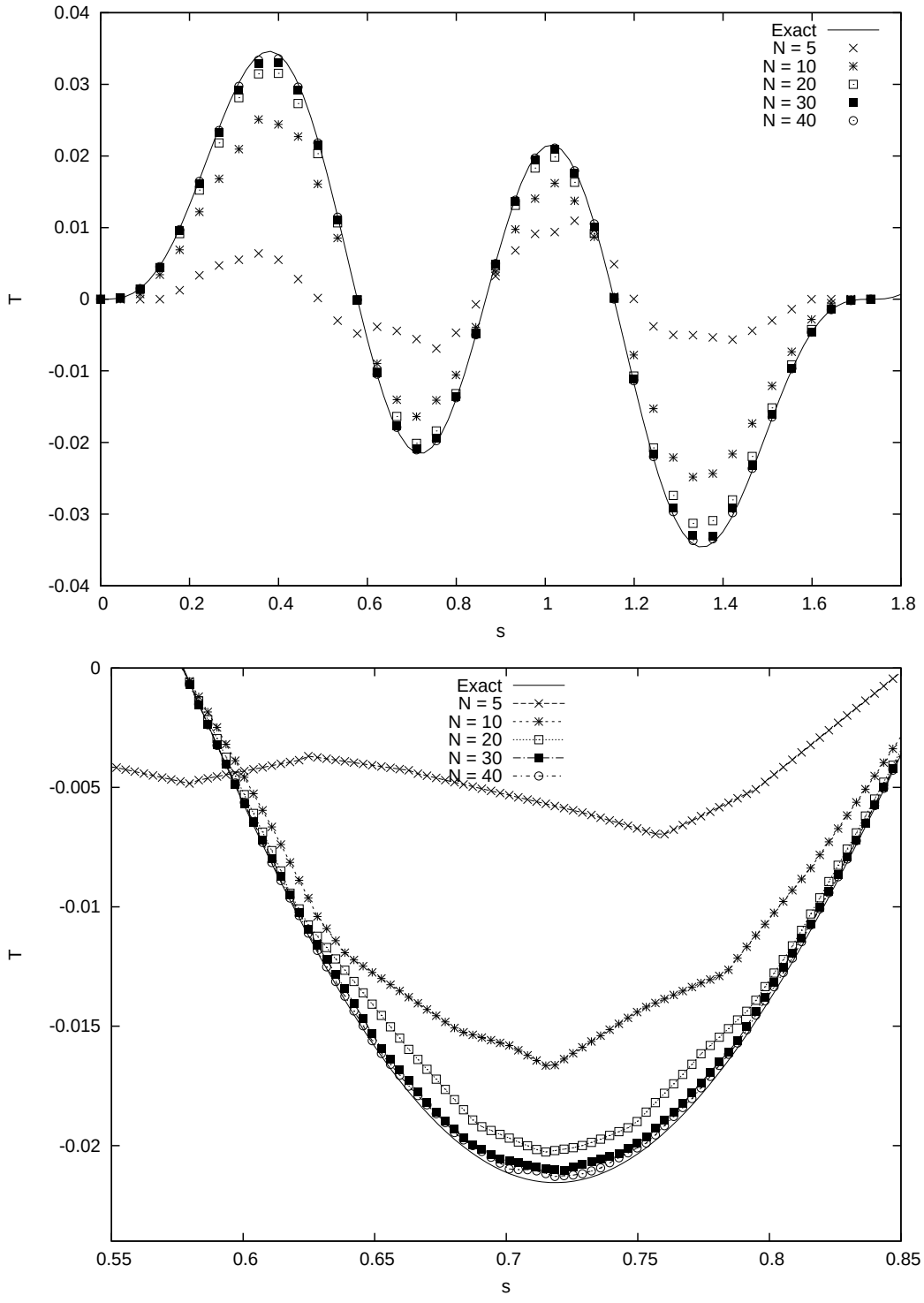

Figure 2.6. Comparison of numerical and exact solutions for various mesh refinement levels for Challenge Problem 11 at $t = 0.02$. Plotted s-values correspond to an equally-spaced interpolation of the numerical solutions along the line from $(0,0,0)$ to $(1,1,1)$ using 40 interpolation points.

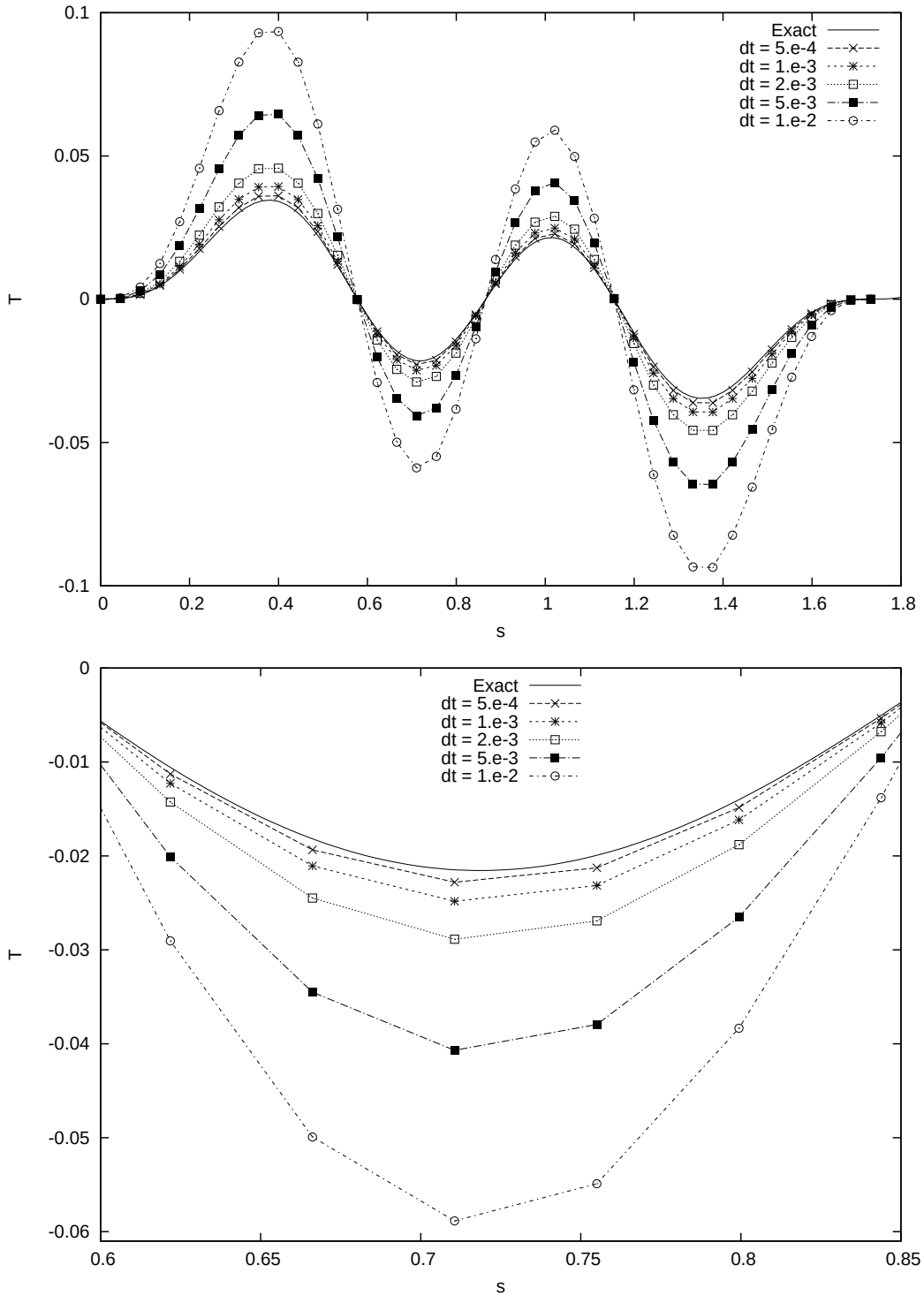

Figure 2.7. Comparison of numerical and exact solutions for various time step sizes for Challenge Problem 11 at $t = 0.02$. Plotted s-values correspond to an equally-spaced interpolation of the numerical solutions along the line from $(0,0,0)$ to $(1,1,1)$ using 40 interpolation points.

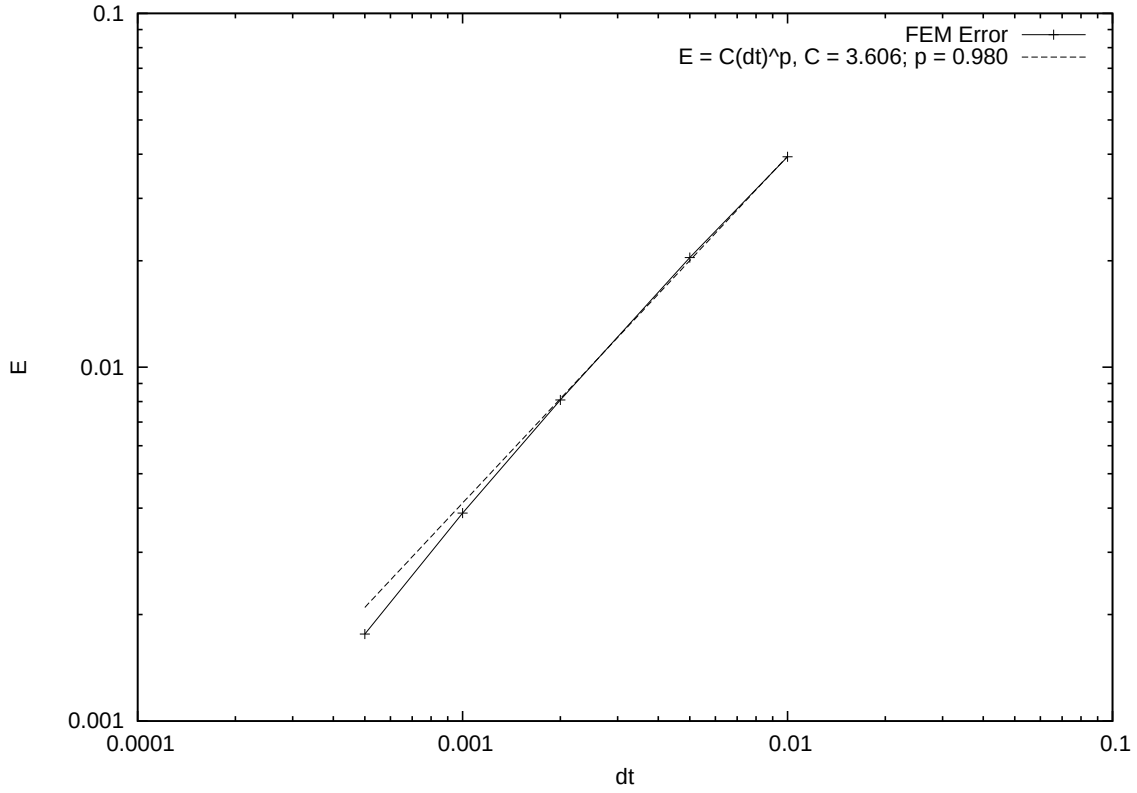

Figure 2.8. Observed Δt order-of-accuracy for Challenge Problem 11. The dashed line is a least-squares fit to the numerical error.

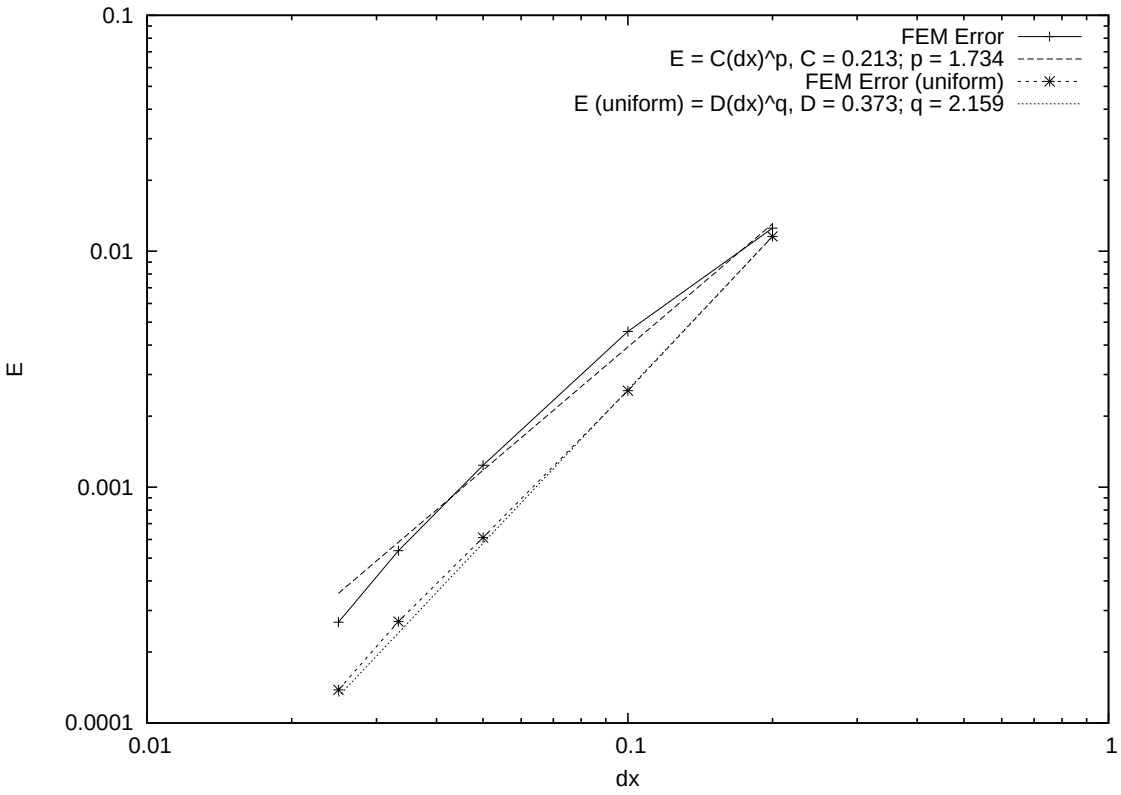

Figure 2.9. Observed Δx order-of-accuracy for Challenge Problem 11. The dashed and dotted lines are least-squares fits to the numerical error.

References

[1] Matthew M. Hopkins, Paul S. Crozier, Russell W . Hooper, Thomas P. Hughes, Jeremiah J. Boerner, Alan B. Williams, Lawrence C. Musson, Steven J. Plimpton, Stan G. Moore, and Matthew T. Bettencourt. Aleph manual. Technical report, Sandia National Laboratories, Dec. 2013.

[2] Thomas J. Hughes. *The Finite Element Method: Linear Static and Dynamic Finite Element Analysis*. Prentice Hall, New Jersey, 1987.

[3] Frank P. Incropera and David P. DeWitt. *Fundamentals of Heat and Mass Transfer*. John Wiley & Sons, New York, 2001.

[4] Patrick Knupp and Kambiz Salari. *Verification of Computer Codes in Computational Science and Engineering*. Chapman and Hall/CRC, New York, 2003.


Sandia National Laboratories